Naval Research Laboratory
Washington, DC 20375-5000

DTIC FILE COPY

NRL Memorandum Report 6532

AD-A222 181

Mode Competition in the Quasioptical Gyrotron

S. RIYOPOULOS,* AND A. W. FLIFLET

Beam Physics Branch
Plasma Physics Division

**Science Applications Int. Corp.*
McLean, VA 22102

May 30, 1990

MAY 3 1 1990

Approved for public release; distribution unlimited.

90 05 29 104

REPORT DOCUMENTATION PAGE

Form Approved
OMB No. 0704-0188

Public reporting burden for this collection of information is estimated to average 1 hour per response, including the time for reviewing instructions, searching existing data sources, gathering and maintaining the data needed, and completing and reviewing the collection of information. Send comments regarding this burden estimate or any other aspect of this collection of information, including suggestions for reducing this burden, to Washington Headquarters Services, Directorate for Information Operations and Reports, 1215 Jefferson Davis Highway, Suite 1204, Arlington, VA 22202-4302, and to the Office of Management and Budget, Paperwork Reduction Project (0704-0188), Washington, DC 20503

1. AGENCY USE ONLY *(Leave blank)*	2. REPORT DATE	3. REPORT TYPE AND DATES COVERED
	1990 May 30	

4. TITLE AND SUBTITLE

Mode Competition in the Quasioptical Gyrotron

5. FUNDING NUMBERS

TA - DE-A105-83
ER52092

6. AUTHOR(S)

Riyopoulos,* S. and Fliflet, A. W.

7. PERFORMING ORGANIZATION NAME(S) AND ADDRESS(ES)

Naval Research Laboratory
Washington, DC 20375-5000

8. PERFORMING ORGANIZATION REPORT NUMBER

NRL Memorandum Report 6532

9. SPONSORING/MONITORING AGENCY NAME(S) AND ADDRESS(ES)

Department of Energy
Washington, DC 20545

10. SPONSORING/MONITORING AGENCY REPORT NUMBER

11. SUPPLEMENTARY NOTES

*Science Applications Intl. Corp., McLean, VA 22102

12a. DISTRIBUTION/AVAILABILITY STATEMENT

Approved for public release; distribution unlimited.

12b. DISTRIBUTION CODE

13. ABSTRACT *(Maximum 200 words)*

A set of equations describing the nonlinear multimode dynamics in the Quasioptical Gyrotron is derived. These equations, involving the slow amplitude and phase variation for each mode, result from an expansion of the nonlinear induced current up to fifth order in the wave amplitude. The interaction among various modes is mediated by coupling coefficients, of known analytic dependence on the normalized current I, the interaction length μ, and the frequency detunings Δ_i corresponding to the competing frequencies ω_i. The particular case when the modes form triads with frequencies $\omega_1 + \omega_3 - 2\omega_2 \equiv 0$ is examined in more detail. The equations are quite general and can be used to study mode competition, the existence of a final steady state, its stability, as well as its accessibility from given initial conditions. It is shown that when $\mu/\beta_\perp >> 1$, μ can be eliminated as an independent parameter. The control space is then reduced to a new normalized current I and the desynchronism parameters $\nu_i = \Delta_i/\mu$ for the interacting frequencies. Each coupling coefficient G_{ij} is written as $G_{ij} = I\, S_{ij}\, G_{ij}(\nu_i, \nu_j)$, where the nonlinear filling factor S_{ij}, carrying the information of the beam current spatial profile, can be computed independently. Therefore, it suffices to compute table of G_{ij} as functions of ν_1, ν_2 and ν_3 once to cover the parameter space. Results for a cold beam are presented here.

14. SUBJECT TERMS		15. NUMBER OF PAGES
Quasioptical Gyrotron Multi-mode Dynamics	Mode competition	65
		16. PRICE CODE

17. SECURITY CLASSIFICATION OF REPORT	18. SECURITY CLASSIFICATION OF THIS PAGE	19. SECURITY CLASSIFICATION OF ABSTRACT	20. LIMITATION OF ABSTRACT
UNCLASSIFIED	UNCLASSIFIED	UNCLASSIFIED	SR

CONTENTS

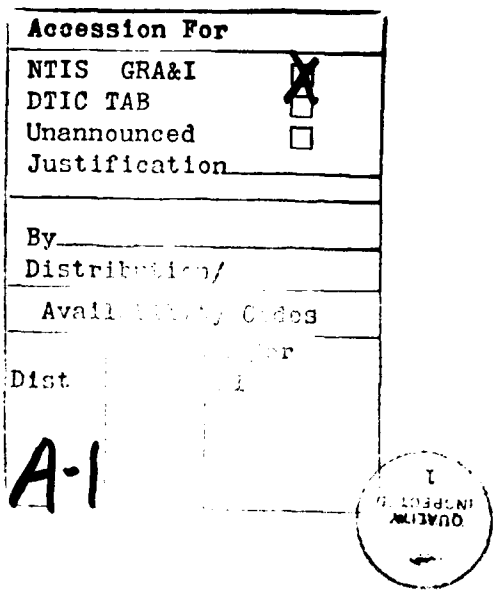

MODE COMPETITION IN THE QUASI-OPTICAL GYROTRON

I. INTRODUCTION

The quasi-optical gyrotron[1-10] (QOG) is a promising millimeter and submillimeter radiation source that has already demonstrated[9] power levels $\lesssim$ 150 kW with pulse durations up to 13 μs at electronic efficiencies $\lesssim$ 14%. Potential applications, ranging from heating of fusion plasmas to short wavelength radars, require stable CW operation at high power levels within a narrow frequency band. Because of the strong fields developed inside the cavity, the high density of longitudinal resonator modes, and the relatively long time of operation, nonlinear interaction among many modes will inevitably occur.[8,9] In fact, it is the nonlinear coupling among cavity modes[11] that will determine the existence of a final steady state, its accessibility from the initial small signal phase, and whether it is a single or a multimode state.

In short, the evolution of the cavity fields can be described as follows. The injected electron beam initially excites all the cavity eigenmodes characterized by a start-up current below the beam current. At small amplitude each mode grows exponentially in time with its linear growth rate, unaffected by the presence of other modes. Soon one or more modes reach finite amplitude and start interacting through the induced modifications in the distribution of the electron beam. When this happens a single mode may nonlinearly suppress all other unstable modes and eventually dominate. Equally well, it may destabilize modes that are linearly stable. In some cases the fastest linearly growing mode may be overtaken by another, linearly slower mode, causing mode switching. The final steady state, if one exists, may involve more than one large amplitude modes. The point to be made here is that the existence of a final steady state, be it single or multimode, is determined nonlinearly

Manuscript approved February 6, 1990.

and cannot be predicted from the linear behavior.

Finding the regimes in parameter space associated with the desired type of final equilibrium proves too costly for direct numerical simulation, given that the performance of the QOG depends on four independent parameters. It should be stressed that the final equilibrium cannot always be obtained by examining the linear stability of every possible single mode at saturation.[10] Even if a saturated single mode is found stable to small perturbations by other modes, there is no guarantee that the system will eventually evolve to this state. In general, more than one stable equilibrium exists for a given set of modes, however, only one of them is accessible from the appropriate initial conditions. In the case that the final steady state is dominated by a single mode, it is not necessarily the mode with the largest linear growth rate. Consequently, all participating modes must be treated on equal basis until (and if) one dominates. Mode selection and accessibility are inherently nonlinear processes.

In this work an analytic model of the multimode dynamics is developed by expanding the nonlinear current in powers of the radiation amplitude. A set of equations is then obtained for the slow time scale evolution of the wave amplitudes and phases. The strength of the nonlinear interactions enters through coupling coefficients of known analytic dependence on the gyrotron parameters. Numerical simulations of particle trajectories are then replaced by a set of first order ordinary differential equations, one for each participating mode. Not only is the computation time reduced by orders of magnitude but, equally important, the final equilibria can be predicted analytically from the coupling coefficients. In this paper we will mainly discuss cases with up to three interacting modes, coupled up to fifth order in the wave amplitude.

The coupled equations obtained here can be applied to the description of phase-locked[12] operation of the QOG through the injection of a small external signal. They can also describe phase locking through the use of a prebunching resonator,[13] via certain modifications resulting from the use of a prebunched injected electron distribution in place of a uniform one.

II. GENERAL FORMALISM

The configuration for the QOG is shown in Fig. 1. The cavity fields are expressed through the vector potential $A(r,t)$,

$$E = -\frac{1}{c}\frac{\partial A}{\partial t}, \qquad B = \nabla \times A, \tag{1}$$

where A is a superposition of eigenmodes of the Fabry-Perot resonator,

$$A(r,t) = \frac{1}{2}\sum_m \tilde{A}_m(t)\, U_m(r)\, e^{-i\omega_m t}\, e_y + cc, \tag{2a}$$

$$U_m(r) = u_{p_m q_m}(r)\cos k_m x . \tag{2b}$$

In the orthogonal coordinates (x,y,z) with x along the resonator axis and z along the electron beam axis, the transverse profiles $u_{pq}(r)$ are given by the Hermite-Gaussian functions

$$u_{p_m q_m}(r) = h_{p_m}(y)\, h_{q_m}(z), \qquad h_{p_m}(z) = H_{p_m}\left(\frac{\sqrt{2}z}{w(x)}\right)\exp\left(-\frac{z^2}{w^2(x)}\right), \tag{3}$$

$w(x) = W\,(1+x^2/b_m^2)^{1/2}$ is the radiation spot size, W is the radiation waist, $b_m = k_m W^2/2$ is the Rayleigh length and $H_p(z)$ are the Hermite polynomials. The wavenumber k_m is equal to ω_m/c, where the cavity frequencies ω_m take the values

$$\omega_m = \frac{\pi c}{L}\left[m-1+\frac{2(p_m+q_m+1)}{\pi}\tan^{-1}\left(\frac{L}{2b}\right)\right] \simeq \frac{\pi c}{L}(m+p_m+q_m), \tag{4}$$

where L is the cavity length and p_m and q_m are integers; the notation p_m, q_m is used for labeling frequencies, $\omega_m \equiv \omega_{mpq}$. According to the weak

coupling approximation, the slowly varying amplitudes $\tilde{A}_m(t)$ are complex quantities with magnitude $A_m(t)$ and phase $\phi_m(t)$,

$$\tilde{A}_m(t) = A_m(t)\, e^{i\phi_m(t)} . \tag{5}$$

The superposition (2), involving various frequencies ω_m, may also contain various modal structures $p_m q_m$ for a given frequency (i.e. degeneracy).

(a) Particle Equations

We use the guiding center description for the transverse particle coordinates

$$\begin{aligned} x &= x_g + \rho \cos\theta , \qquad y = y_g + \rho \sin\theta , \\ p_x &= p_{gx} - p_\perp \sin\theta , \quad p_y = p_{gy} + p_\perp \cos\theta , \end{aligned} \tag{6}$$

where (x_g, y_g) and (p_{gx}, p_{gy}) denote the guiding center position and momentum, $p_\perp$ is the magnitude of the transverse momentum, θ is the gyroangle, $\rho = p_\perp/\Omega_c$ is the Larmor radius, $\Omega_c = \Omega_o/\gamma$ is the relativistic cyclotron frequency, where $\Omega_o = |e|B_o/mc$, and the relativistic factor $\gamma = [1 + (p_\perp/mc)^2 + (p_z/mc)^2]^{1/2}$. By averaging the exact Lorentz force equations in the vector potential representation over the fast (cyclotron) time scale, the slow-time-scale nonlinear relativistic equations of motion are cast in the form

$$\frac{du_\perp}{dt} = \sum_n \omega_n a_n J_1'(k_n\rho) \sin(\psi_n + \phi_n) \cos k_n x_g , \tag{7a}$$

$$\frac{d\theta}{dt} = \frac{\Omega_o}{\gamma} + \sum_n \frac{\omega_n}{u_\perp} a_n \frac{J_1(k_n\rho)}{k_n\rho} \cos(\psi_n + \phi_n) \cos k_n x_g . \tag{7b}$$

In Eqs. (7) time has been normalized to $\omega_o^{-1} \equiv (\Omega_o/\gamma_o)^{-1}$, length to $k_o^{-1} = c/\omega_o$, $a_n = |e|A_n/mc^2$ is the normalized radiation amplitude, u is the normalized momentum $u = p/mc = \gamma v/c$ and the relativistic factor $\gamma = (1 + u_\perp^2 + u_z^2)^{1/2}$. The angle ψ_m is the relative phase between the m-th mode and the particle, $\psi_m = \theta - \omega_m t$, evolving in time as

$$\frac{d\psi_n}{dt} = - \delta\omega_n + \sum_n \frac{\omega_n}{u_\perp} a_n \frac{J_1(k_n\rho)}{k_n\rho} \cos(\psi_n + \phi_n) \cos k_n x_g , \qquad (8)$$

where $\delta\omega_n = (\omega_n - \Omega_o/\gamma_o)\ \omega_o^{-1}$ is the zero-order frequency detuning. The prime (′) signifies the Bessel function derivative in respect to the argument. The evolution of γ is found combining Eqs. (7a) to (7b), to obtain

$$\frac{d\gamma}{dt} = \sum_n \omega_n \frac{u_\perp}{\gamma} a_n J_1'(k_n\rho) \sin(\psi_n + \phi_n) \cos k_n x_g . \qquad (9)$$

Two approximations are implicit in Eqs. (7)-(9). The guiding center drift has been ignored and the axial relativistic momentum u_z is taken as constant. They are both justified for $a_n << 1$, $kW >> 1$, since $dx_g/dt \sim dy_g/dt \sim O(a_n^2)$ and $du_z/dt \sim O(a_n/kW)$, which are much smaller than $du/dt \sim d\theta/dt \sim O(a_n)$.

(b) Field Equations

Substituting Eq. (2) into Maxwell's equations and ignoring second order derivatives $\partial^2\tilde{A}_n/\partial t^2 << \omega_n^2\tilde{A}_n$, the slow-time evolution of the vector potentials is given by

$$\sum_n \left\{ i\omega_n \frac{\partial \tilde{A}_n}{\partial t} U_n e^{-i\omega_n t} + cc \right\} = \frac{4\pi}{c} j_{NL} - \sum_n \left\{ \tilde{A}_n \left(\nabla^2 - \frac{1}{c^2} \frac{\partial^2}{\partial t^2} \right) U_n e^{-i\omega_n t} + cc \right\}. \tag{10}$$

The second term in the right-hand side of Eq. (10) is zero by definition for the vacuum eigenmodes defined in Eq. (2b), thus, all the information for the slow evolution of the fields is carried in the nonlinear transverse current j_{NL}. Equation (10) can also be derived from the general expression governing coherent wave interaction,[14]

$$\left(\frac{\partial \varepsilon}{\partial \omega}\right)_n \left[\frac{\partial}{\partial t} - v_g \frac{\partial}{\partial x} \right] \tilde{A}_n = \frac{4\pi i}{c} j_{NL} , \tag{11}$$

in the limit of standing waves inside the resonator (zero group velocity, $v_g = 0$) and near vacuum dielectric constant ε (weak beam limit: $\omega_b^2/\omega_o^2 \ll 1$), $(d\varepsilon/d\omega)_n \simeq 2\omega_n$.

Multiplying both sides of Eq. (10) by $\exp(i\omega_n t)$ and taking the fast time average over $\tau_o \sim 2\pi/\omega_o$ isolates the n^{th} mode on the left-hand side. Introducing the normalized variables used in Eqs. (7), and letting $\tilde{a}_n \equiv |e|\tilde{A}_n/mc = a_n \exp(i\phi_n)$, we have

$$U_n(r) \frac{\partial \tilde{a}_n}{\partial t} = - \frac{i\, 4\pi |e|}{2\omega_o^2 mc^3} j_{NL}(r;\omega_n) , \tag{12a}$$

where

$$j_{NL}(r;\omega_n) \equiv \frac{1}{\tau_o} \int_0^{\tau_o} dt\, j_{NL}(r,t)\, e^{i\omega_n t} . \tag{12b}$$

Multiplying both sides by the mode profile U_n and integrating over the cavity volume lead to

$$\left(\frac{\partial}{\partial t} - \frac{\omega_n}{2Q_n} \right) \tilde{a}_n = - \frac{i\, 2\pi |e|}{\omega_o^2 mc^3 V_n} \int d^3r\, U_n(r)\, j_{NL}(r;\omega_n) \ . \qquad (13)$$

Above $V_n = \int d^3r \ \ U_n^2$ is the weighted cavity volume, and the phenomenological term ω_n/Q_n was added to account for resonator losses due to boundary effects, where the cavity Q_n is defined by

$$\frac{d}{dt} a_n^2 = - \frac{\omega_n}{Q_n} a_n^2 \ . \qquad (14)$$

The current is expressed in terms of the nonlinear distribution function f_{NL},

$$j_{NL}(r,t) = -|e|\, n_b(r) \int_0^{2\pi} d\theta \int_0^{\infty} du_z \int_0^{\infty} du_\perp u_\perp \frac{u_\perp}{\gamma} \cos\theta\, f_{NL}(r,u,t) \ . \qquad (15)$$

Letting $f_{NL}(r,u,t) = n_o \ \hat{n}_b(r_\perp) \ \ f_{NL}(u_\perp,u_z,z;t)$, substituting (15) in Eq. (13), and expressing $r_\perp \equiv (x,y)$ and $u_\perp \equiv (u_x,u_y)$ in the guiding center representation Eq. (6), the right-hand side of Eq. (15) becomes

$$-i \frac{2\pi\, c\, |e|\, n_o}{\omega_o^2\, mc^3\, V_m} \int_0^L dx_g \int_{-\infty}^{\infty} dy_g \int_{-\infty}^{\infty} dz\, \hat{n}_b(x_g,y_g)\, h_{p_n}(y_g)\, h_{q_n}(z) \cos k_n x_g$$

$$\int_0^{2\pi} d\theta \int_0^{\infty} du_z \int_0^{\infty} du_\perp u_\perp \frac{u_\perp}{\gamma} \cos\theta\, J_1'(k_n \rho)\, f_{NL}(u_\perp,u_z,\theta,z;\omega_n) \ , \qquad (16)$$

where again $f_{NL}(r;\omega_n) = (1/\tau_o) \int_o^{\tau} dt\, f_{NL}(r,t) \exp(i\omega_n t)$. Expression (16) is finally recast in terms of the injected beam current

$$I_b = |e|\, c\beta_{zo} n_o \int dx_g \int dy_g\, \hat{n}_b(x_g, y_g) \ , \tag{17}$$

as

$$\left(\frac{\partial}{\partial t} - \frac{\omega_n}{2Q_n}\right) \tilde{a}_n = -\, 2\pi i \, \langle j_{NL}(\omega_n) \rangle \ . \tag{18}$$

The dimensionless, volume averaged current on the right-hand side of Eq. (18),

$$\langle j_{NL}(\omega_n)\rangle \equiv \frac{\gamma}{u_z} \frac{I_o}{\sigma_b V_n} \frac{1}{\tau_o} \int_0^{\tau_o} dt\, e^{i\omega_n t} \int_V dr\, U(r)\, j_{NL}(r,t)$$

$$= \frac{\gamma}{u_z} \frac{I_o}{\sigma_b V_n} \int_V dr\, U_n(r)\, j_{NL}(r;\omega_n) \tag{19a}$$

is given, in terms of f_{NL} from Eq. (16), by

$$\langle j_{NL}(\omega_n)\rangle \equiv \frac{I_o}{\sigma_b V_n} \frac{\gamma}{u_z} \int_0^L dx_g \int_{-\infty}^{\infty} dy_g\, \hat{n}_b(x_g, y_g)\, h_{p_n}(y_g) \cos k_n x_g$$

$$\int_{-\infty}^{\infty} dz\, h_{q_n}(z) \int_0^{2\pi} d\theta \int_0^{\infty} du_z \int_0^{\infty} du_\perp u_\perp\, J_1'(k_n \rho)\, \frac{u_\perp}{\gamma} \cos\theta\, f_{NL}(u_\perp, u_z, \theta, z; \omega_n) \ , \tag{19b}$$

where $I_o = |e| I_b / mc^3$ is the dimensionless beam current (Budker parameter), and $\sigma_b = \iint dx_g dy_g\, \hat{n}_b(x_g, y_g)$ is the effective beam cross section.

III. NONLINEAR ELECTRON DISTRIBUTION

The nonlinear electron distribution in phase space $f_{NL}(u_\perp, u_z, \theta, z, t)$ will be obtained in the form of an asymptotic expansion in powers of the small amplitudes $a_n << 1$. Once the form of f_{NL} in the multimode field (2) is known, the nonlinear transverse current j_{NL} is obtained from Eq. (19). The evolution of f_{NL} along the particle trajectories Eqs. (7) is given by the collisionless kinetic equation

$$\frac{\partial f_{NL}}{\partial t} + u_z \frac{\partial f_{NL}}{\partial z} + \frac{d\theta}{dt}\frac{\partial f_{NL}}{\partial \theta} + \frac{du_z}{dt}\frac{\partial f_{NL}}{\partial u_z} + \frac{du_\perp}{dt}\frac{\partial f_{NL}}{\partial u_\perp} = 0. \tag{20}$$

By formally expanding f_{NL} and ordering in powers of a^j, $a \sim O(a_n) << 1$

$$f_{NL} = f^{(0)} + a\, f^{(1)} + \ldots + a^j f^{(j)} ,$$

one obtains a hierarchy of equations

$$L_o f^{(j)} = L_1 f^{(j-1)} \equiv D f^{(j-1)} , \tag{21}$$

where

$$L_o = \frac{\partial}{\partial t} + u_z \frac{\partial}{\partial z} + \Omega_c \frac{\partial}{\partial \theta} , \tag{22a}$$

$$L_1 = \sum\nolimits^{\sim} a_n \left\{ \frac{1}{2i} J_1'(k_n\rho) \cos k_n x_g\, e^{i\psi_n} \frac{\partial}{\partial u_\perp} + \frac{1}{2u_\perp} \frac{J_1(k_n\rho)}{k_n\rho} \cos k_n x_g\, e^{i\psi_n} \frac{\partial}{\partial \theta} \right\}. \tag{22b}$$

Operator L_o is the total time derivative $L_o \equiv d/dt$ along the unperturbed orbits of electrons gyrating in the external magnetic field B_o

$$\theta' = \theta - \Omega_c \tau \ , \quad u_\perp' = u_\perp \ , \quad z' = z - \frac{u_z}{\gamma}\tau \ , \quad \psi_n' = \psi_n - \delta\omega_n \tau \ , \quad (23)$$

(the characteristic curves of $L_o f = 0$ in the theory of partial differential equations) where $\theta' \equiv \theta(t')$, $\theta \equiv \theta(t)$ and $\tau = t - t'$. Replacing the exact trajectories in the right-hand side of (21) by the unperturbed orbits (23), (integration along the characteristics), it follows that

$$f^{(j)} = \int_0^\infty d\tau \, Df^{(j-1)} \left[u'(\tau), \, \theta'(\tau), \, z'(\tau) \right] , \qquad (24)$$

We exploit the fact that the interaction time of an electron inside the cavity, of the order of the transit time $t_i \simeq W/\beta_z$, is much shorter than the characteristic growth time $t_c^{-1} = d(\ln a_m)/dt$ for the fields. Keeping $\tilde{a}_n$ constant during the integration (24) yields

$$f^{(j)} = \sum_n \tilde{a}_n \sin k_n x_g \, e^{i(\theta - \omega_n t_j)} \qquad (25)$$

$$\int_0^\infty d\tau_j \, h_n\left(z - \frac{u_z \tau_j}{\gamma}\right) e^{i\delta\omega_n \tau_j} \left(\frac{J_1'(k_n\rho)}{2i} \frac{\partial}{\partial u_\perp} + \frac{J_1(k_n\rho)}{(k_n\rho)} \frac{1}{2u_\perp} \frac{\partial}{\partial \theta} \right) f^{(j-1)} + cc,$$

where $\tau_j \equiv t_j - t_{j-1}$ and we used

$$\psi_n(t_{j-1}) = \theta(t_{j-1}) - \omega_n t_{j-1} = \theta_j - \omega_n t_j + \delta\omega_n \tau_j \ .$$

It is now convenient to change variables, introducing the set ζ_o, ζ_1, ... , ζ_j, defined by

$$\zeta_o = \frac{z}{W} \ , \quad \zeta_1 = \zeta_o - \frac{u_z}{\gamma W}\tau_1 \ , \ \ldots \ , \quad \zeta_j = \zeta_{j-1} - \frac{u_z}{\gamma W}\tau_j = \frac{z}{W} - \frac{u_z}{\gamma W}(\tau_1 + \tau_2 + \ldots + \tau_j) \qquad (26)$$

where $d\zeta_j = -(u_z/\gamma W)\, d\tau_j$ and $\zeta_j(\tau_j = 0) = \zeta_{j-1}$. Successive iterations of Eq. (25) yield

$$f^{(j)} = \int_0^\infty d\tau_1 L_1(\tau_1) \int_0^\infty d\tau_2 L_1(\tau_2) \int_0^\infty \cdots\cdots \int_0^\infty d\tau_j\, L_1(\tau_j)\, f^{(0)}$$

$$= (-1)^j \left(\frac{\gamma W}{u_z}\right)^j \int_{-\infty}^{\zeta_0} d\zeta_1 L_1(\zeta_1) \int_{-\infty}^{\zeta_1} d\zeta_2 L_1(\zeta_2) \int_{-\infty}^{\zeta_2} \cdots\cdots \int_{-\infty}^{\zeta_{j-1}} d\zeta_j\, L_1(\zeta_j)\, f^{(0)}\,, \tag{27}$$

where $f^{(0)}$ is the injected beam distribution, and L_1 is written as

$$\int_{-\infty}^{\zeta_{j-1}} d\zeta_j\, L_1(\zeta_j) \equiv \sum_n \tilde{a}_n\, e^{i(\theta - \omega_n t_j + \nu_n t_j)} \cos k_n x_g$$

$$\int_{-\infty}^{\zeta_{j-1}} d\zeta_j\, h_n(\zeta_j)\, e^{i\nu_n \zeta} \left(\frac{J_1'(k_n\rho)}{2i} \frac{\partial}{\partial u_\perp} + \frac{J_1(k_n\rho)}{(k_n\rho)} \frac{1}{2u_\perp} \frac{\partial}{\partial \theta} \right) + \text{cc}\,. \tag{28}$$

The quantity $\nu_n = (W\gamma/u_z)\,\delta\omega_n$, the product of the frequency detuning times the transit time through the cavity is the most important parameter for the mode coupling coefficients. The integrations, Eqs. (27) and (28), are carried out in Appendix A. The expressions for $f^{(j)}$, $j=1,2,3$ are given by (A1)-(A3). For $j \geq 4$ the full expressions are getting rather complicated. However, one may exploit the existing ordering inside $f^{(j)}$ in powers of the large parameter $\eta = (kW/\gamma)(u_\perp/u_z) \gg 1$. It is then easier to find an approximation for $f^{(j)}$ to any order in j, Eq. (A6), by keeping the dominant contribution. Additional simplifications occur during the gyroangle averaging in obtaining the nonlinear current, given by Eqs. (A7) and (A8).

IV. MODE COUPLING EQUATIONS

Substituting expression (A7) for the nonlinear current inside the right hand side of Eq. (A8) and keeping terms up to fifth order in complex amplitudes $\tilde{a}_m = a_m \exp(i\phi_m)$, the general mode coupling equations assume the form

$$\frac{d\tilde{a}_n}{dt} = - \frac{2\pi i \gamma_o I_o}{u_{zo} \sigma_b V_n} \sum_{\{i,j,\ldots,m\}}^{\Delta} \left(C^{(1)}_{m;n} \tilde{a}_m + C^{(3)}_{klm;n} \tilde{a}_k \tilde{a}_l \tilde{a}_m + C^{(5)}_{ijklm;n} \tilde{a}_i \tilde{a}_j \tilde{a}_k \tilde{a}_l \tilde{a}_m \right) . \quad (29)$$

A mode of given frequency ω_n interacts through all possible frequency combinations satisfying the resonant condition

$$\Delta\omega_{ij\ldots m;n} \equiv (\omega_i \pm \omega_j \pm \cdots \pm \omega_m) - \omega_n \simeq 0 , \quad (30)$$

denoted by $\sum^{\Delta}$; the notation {i,j,...,m} implies summation over all permutations among i,j,...,m (except n) inside Eq. (29), for a given set of resonant frequencies (30). A negative index -m will imply $-\omega_m$, $-\phi_m$, $-\nu_m$ and $\tilde{a}_n^*$ in place of ω_m, ϕ_m, ν_m and $\tilde{a}_n$ respectively.

The dominant contribution to the coupling coefficients $C^{(j)}$ is given by

$$C^{(1)}_{m;n} = \left(\frac{i}{2}\right) W^2 S_{m;n} \int_0^{\infty} du_\perp \frac{u_\perp^2}{\gamma} \left(\frac{\gamma}{u_{zo}}\right) \int_{-\infty}^{\infty} dz \, v_n(z) \int_{-\infty}^{z} d\zeta_1 \, v_m(\zeta_1) \frac{df^{(0)}}{du_\perp} , \quad (31a)$$

$$C^{(3)}_{klm;n} = \left(\frac{i}{2}\right)^3 W^4 S_{klm;n} \exp\left[i\left(\Delta\omega_{klm;n}t + \Phi_{klm;n}\right)\right] \int_0^\infty du_\perp \frac{u_\perp^2}{\gamma}\left(\frac{\gamma}{u_{zo}}\right)^3$$

$$\times \int_{-\infty}^{\infty} dz\, v_n(z) \int_{-\infty}^{z} d\zeta_1\, v_k(\zeta_1) \frac{\partial}{\partial u_\perp} \int_{-\infty}^{\zeta_1} d\zeta_2\, v_l(\zeta_2) \frac{\partial}{\partial u_\perp} \int_{-\infty}^{\zeta_2} d\zeta_3\, v_m(\zeta_3) \frac{df^{(0)}}{du_\perp}, \tag{31b}$$

$$C^{(5)}_{ijklm;n} = \left(\frac{i}{2}\right)^5 W^6 S_{ijklm;n} \exp\left[i\left(\Delta\omega_{ijklm;n}t + \Phi_{ijklm;n}\right)\right] \int_0^\infty du_\perp \frac{u_\perp^2}{\gamma}\left(\frac{\gamma}{u_{zo}}\right)^5$$

$$\int_{-\infty}^{\infty} dz\, v_n(z) \int_{-\infty}^{z} d\zeta_1\, v_i(\zeta_1) \frac{\partial}{\partial u_\perp} \int_{-\infty}^{\zeta_1} d\zeta_2\, v_j(\zeta_2) \frac{\partial}{\partial u_\perp} \int_{-\infty}^{\zeta_2} \cdots \frac{\partial}{\partial u_\perp} \int_{-\infty}^{\zeta_4} d\zeta_5\, v_m(\zeta_5) \frac{df^{(0)}}{du_\perp}, \tag{31c}$$

where

$$v_m(\zeta) \equiv J_1'(k_m\rho)\, h_m(\zeta)\, e^{-i\nu_m\zeta}, \tag{32}$$

$\Phi_{ij\ldots m;n} \equiv (\phi_i \pm \phi_j \pm \cdots \pm \phi_m) - \phi_n$ is the combined slow phase, and the nonlinear filling factor is given by

$$S_{ij\ldots m;n} = 2\int_0^{\frac{L}{2}} dx_g \int_{-\infty}^{\infty} dy_g\, \hat{n}_b(x_g,y_g) \left(1 + \frac{x_g^2}{b_i^2}\right)^{-\frac{1}{2}} \left(1 + \frac{x_g^2}{b_j^2}\right)^{-\frac{1}{2}} \cdots \left(1 + \frac{x_g^2}{b_n^2}\right)^{-\frac{1}{2}}$$

$$h_i(y_g)\, h_j(y_g) \ldots h_n(y_g) \cos k_i x_g \cos k_j x_g \cdots \cos k_n x_g. \tag{33}$$

The results appearing in Eqs. (29)-(33) apply for any spatial profile and velocity distribution of the electron beam, as well as any radiation modal structure in the open resonator.

V. THREE MODE INTERACTION

Equations (29) are quite general, involving all possible resonant combinations of modes. In many cases it has been observed that only a small number of modes participates in the final equilibrium with finite amplitude. In this section the three mode synchronous interaction, satisfying the condition

$$\nu_k + \nu_l \simeq 2\nu_m \ , \quad \text{or} \quad \omega_k + \omega_l \simeq 2\omega_m \ , \tag{34}$$

will be considered in more detail. This is a special case of the four mode interaction, with $\omega_m = \omega_n$ in Eq. (30). Hence the frequencies ω_k, ω_l are symmetric around ω_m, $\omega_k = \omega_m - d\omega$, $\omega_l = \omega_m + d\omega$, where $d\omega$ is any frequency interval allowed by the mode spacing in the cavity. The possible resonant frequency triads entering $C^{(3)}$ are

$$\begin{aligned} &\omega_m - \omega_l - \omega_k \ , \\ -&\omega_m - \omega_l + \omega_l \ , \\ -&\omega_m - \omega_k + \omega_k \ , \\ -&\omega_m - \omega_m + \omega_m \ , \end{aligned} \tag{35}$$

and all 3! permutations of each arrangement, while the possible arrangements for $C^{(5)}$ are given, setting $i = k$ and $j = l$, by

$$\begin{aligned} -&\omega_m - \omega_l + \omega_l - \omega_k + \omega_k \ , \\ -&\omega_m - \omega_k + \omega_k - \omega_m + \omega_m \ , \\ -&\omega_m - \omega_m + \omega_m - \omega_m + \omega_m \ , \\ &\omega_m - \omega_l - \omega_k + \omega_k - \omega_k \ , \\ &\omega_m - \omega_l - \omega_k + \omega_l - \omega_l \ , \\ &\omega_m - \omega_l - \omega_k + \omega_m - \omega_m \ , \end{aligned} \tag{36}$$

with all the 5! permutations of each.

There has been a tendency recently to employ the following renormalized parameters in gyrotron theory: amplitude $F_n = a_n/\gamma_o\beta_{\perp o}{}^3 = E_n/B_o\beta_{o\perp}{}^3$, detuning $\Delta_n = (2/\beta_{\perp o}{}^2)\delta\omega_n$, interaction length $\mu = k_o W(\beta_{\perp o}{}^2/2\beta_{zo})$ and current $I = I_o\,(8\pi/V_o)(Q/\gamma_o\beta_{\perp o}{}^3)$ where $V_o = (\pi/2)k_o{}^3 LW^2$ and $I_o = I_b(\text{Ams})|e|/m_e c^3 \times 3\ 10^9$. Setting $\omega_k = \omega_1$, $\omega_m = \omega_2$, $\omega_l = \omega_3$ and separating real and imaginary parts, Eqs. (29) are recast in the form

$$\frac{dF_1}{dt} + \frac{\omega_1}{2Q_1} F_1 = \mathrm{Re}\Gamma_1 F_1 + \sum_{m=1}^{3} F_1 F_m{}^2 \mathrm{Re}G_{1m} + F_2{}^2 F_3 \mathrm{Re}\left(G_{123}\, e^{-i\Phi}\right)$$

$$+ \sum_{l=1}^{3}\sum_{m=1}^{3} F_1 F_l{}^2 F_m{}^2 \mathrm{Re}D_{11m} + \sum_{m=1}^{3} F_m{}^2 F_2{}^2 F_3 \mathrm{Re}\left(D_{m123}\, e^{-i\Phi}\right), \quad (37a)$$

$$\frac{dF_2}{dt} + \frac{\omega_2}{2Q_2} F_2 = \mathrm{Re}\Gamma_2 F_2 + \sum_{m=1}^{3} F_2 F_m{}^2 \mathrm{Re}G_{2m} + F_1 F_2 F_3 \mathrm{Re}\left(G_{231}\, e^{i\Phi}\right)$$

$$+ \sum_{l=1}^{3}\sum_{m=1}^{3} F_2 F_l{}^2 F_m{}^2 \mathrm{Re}D_{21m} + \sum_{m=1}^{3} F_m{}^2 F_1 F_2 F_3 \mathrm{Re}\left(D_{m231}\, e^{i\Phi}\right), \quad (37b)$$

$$\frac{dF_3}{dt} + \frac{\omega_3}{2Q_3} F_3 = \mathrm{Re}\Gamma_3 F_3 + \sum_{m=1}^{3} F_3 F_m{}^2 \mathrm{Re}G_{1m} + F_2{}^2 F_1 \mathrm{Re}\left(G_{312}\, e^{-i\Phi}\right)$$

$$+ \sum_{l=1}^{3}\sum_{m=1}^{3} F_3 F_l{}^2 F_m{}^2 \mathrm{Re}D_{31m} + \sum_{m=1}^{3} F_m{}^2 F_2{}^2 F_1 \mathrm{Re}\left(D_{m312}\, e^{-i\Phi}\right), \quad (37c)$$

where Γ is the complex linear growth rate. The evolution of the slow phase $\Phi = \phi_1 + \phi_3 - 2\phi_2$ is given by

$$\frac{d\Phi}{dt} = \delta\Omega + \mathrm{Im}\left(\Gamma_1 + \Gamma_3 - 2\,\Gamma_2\right)$$

$$- F_1^{\,2}\mathrm{Im}\left(G_{11} + G_{31} - 2G_{21}\right) - F_3^{\,2}\mathrm{Im}\left(G_{13} + G_{33} - 2G_{23}\right) + F_2^{\,2}\mathrm{Im}\left(G_{22} - G_{12} - G_{32}\right)$$

$$- \frac{F_3\,F_2^{\,2}}{F_1}\,\mathrm{Im}\left(G_{123}\,e^{\,i\Phi}\right) - \frac{F_1\,F_2^{\,2}}{F_3}\,\mathrm{Im}\left(G_{312}\,e^{\,i\Phi}\right) + F_1\,F_3\,\mathrm{Im}\left(G_{231}\,e^{-\,i\Phi}\right)$$

$$- \sum_{l=1}^{3}\sum_{m=1}^{3}\mathrm{Im}\left(D_{11m} + D_{31m} - 2D_{21m}\right)F_1^{\,2}\,F_m^{\,2}$$

$$- \sum_{m=1}^{3}F_m^{\,2}\left\{\frac{F_3\,F_2^{\,2}}{F_1}\,\mathrm{Im}\left(D_{m123}e^{\,i\Phi}\right) + \frac{F_1\,F_2^{\,2}}{F_3}\,\mathrm{Im}\left(D_{m312}e^{\,i\Phi}\right) - F_1\,F_3\,\mathrm{Im}\left(D_{m231}e^{-\,i\Phi}\right)\right\}, \tag{37d}$$

where $\delta\Omega = (\omega_1 + \omega_3 - 2\omega_2)/\omega_o$. Note that only one combined slow phase appears for each triad.

The dependence on the gyrotron parameters I, μ and Δ is contained in the coupling coefficients. It will be shown now that when $\mu >> \gamma_o\beta_{\perp o}/2$, it can be eliminated as an independent parameter by proper scaling. The computation of Γ, G, and D, carried out in Appendix B, yields

$$\begin{aligned} \Gamma_n &= I_s S_1\,\hat{\Gamma}(\nu_n)\,, \\ G_{nm} &= I_s S_3\,\xi^2\,\hat{G}(\nu_n,\nu_m)\,, \\ D_{nml} &= I_s S_5\,\xi^4\,\hat{D}(\nu_n,\nu_m,\nu_l)\,, \end{aligned} \tag{38}$$

where $\xi = (k_o W)^2(\beta_{\perp o}^{\,4}/2\beta_{zo}^{\,2})J_1'(k_o\rho_o)$ and $I_s = I(\beta_{\perp o}^{\,2}/8Q)(k_o W)^3(\beta_{\perp o}/\beta_{zo})^3[J_1'(k_o\rho_o)]^2$. The nonlinear filling factors S_1, S_3, and S_5 are given in (B11). The quantities $\hat{\Gamma}$, $\hat{G}$, $\hat{D}$,given for a cold beam by the integrals (B16)-(B18), depend on the desynchronism parameter

ν_m alone, the product of the interaction length μ with the detuning Δ_m,

$$\nu_m = \mu \Delta_m \ . \tag{39}$$

This suggests the following scaling transformation, valid when $\omega_n \approx \omega_o$ and $Q_n \approx Q$,

$$\begin{aligned} \dot{I} &= 2 I_s Q \\ \dot{F} &= \xi F \ , \\ \tau &= t/2Q \ , \end{aligned} \tag{40}$$

putting the mode coupling equations in the final reduced form

$$\frac{d\dot{F}_1}{d\tau} + \dot{F}_1 = \dot{I}\left\{S_1 \mathrm{Re}\dot{\Gamma}_1 \dot{F}_1 + S_3 \sum_{m=1}^{3} \dot{F}_1 \dot{F}_m^{\,2} \mathrm{Re}\dot{G}_{1m} + S_3 \dot{F}_2^{\,2} \dot{F}_3 \, \mathrm{Re}\left(\dot{G}_{123}\, e^{-i\Phi}\right)\right.$$

$$\left. + S_5 \sum_{l=1}^{3} \sum_{m=1}^{3} \dot{F}_1 \dot{F}_l^{\,2} \dot{F}_m^{\,2} \mathrm{Re}\dot{D}_{11m} + S_5 \sum_{m=1}^{3} \dot{F}_m^{\,2} \dot{F}_2^{\,2} \dot{F}_3 \, \mathrm{Re}\left(\dot{D}_{m123}\, e^{-i\Phi}\right)\right\} , \tag{41a}$$

$$\frac{d\dot{F}_2}{d\tau} + \dot{F}_2 = \dot{I}\left\{S_1 \mathrm{Re}\dot{\Gamma}_2 \dot{F}_2 + S_3 \sum_{m=1}^{3} \dot{F}_2 \dot{F}_m^{\,2} \mathrm{Re}\dot{G}_{2m} + S_3 \dot{F}_1 \dot{F}_2 \dot{F}_3 \, \mathrm{Re}\left(\dot{G}_{123}\, e^{i\Phi}\right)\right.$$

$$\left. + S_5 \sum_{l=1}^{3} \sum_{m=1}^{3} \dot{F}_2 \dot{F}_l^{\,2} \dot{F}_m^{\,2} \mathrm{Re}\dot{D}_{21m} + S_5 \sum_{m=1}^{3} \dot{F}_m^{\,2} \dot{F}_1 \dot{F}_2 \dot{F}_3 \, \mathrm{Re}\left(\dot{D}_{m231}\, e^{i\Phi}\right)\right\} , \tag{41b}$$

$$\frac{d\dot{F}_3}{d\tau} + \dot{F}_3 = \dot{I}\left\{S_1 \mathrm{Re}\dot{\Gamma}_3 \dot{F}_3 + S_3 \sum_{m=1}^{3} \dot{F}_3 \dot{F}_m^{\,2} \mathrm{Re}\dot{G}_{3m} + S_3 \dot{F}_2^{\,2} \dot{F}_1 \, \mathrm{Re}\left(\dot{G}_{312}\, e^{-i\Phi}\right)\right.$$

$$\left. + S_5 \sum_{l=1}^{3} \sum_{m=1}^{3} \dot{F}_3 \dot{F}_l^{\,2} \dot{F}_m^{\,2} \mathrm{Re}\dot{D}_{31m} + S_5 \sum_{m=1}^{3} \dot{F}_m^{\,2} \dot{F}_2^{\,2} \dot{F}_1 \, \mathrm{Re}\left(\dot{D}_{m312}\, e^{-i\Phi}\right)\right\} . \tag{41c}$$

It follows, from (41), that the normalized start-up current is $\dot{I}_n = 1/S_1\dot{\Gamma}_n$.

The beam parameters I, β_{zo}, $\beta_{\perp o}$ the interaction length μ, the cavity Q and the three frequencies combine into only 3 control parameters: $\hat{I}$, ν_1 and ν_2 (ν_3 is related to the other two frequencies through the resonant condition). The interaction length μ does not appear explicity, but only implicitly through $\hat{I}$ and ν. For simple density profiles, such as a pencil or a thin annular beam, the filling factors may also be expressed as powers of a single factor s,

$$S_j = s^{j+1} , \qquad s = \cos k_o \bar{x}_g \; h(\bar{y}_g) , \tag{42}$$

with $\bar{x}_g$ and $\bar{y}_g$ the effective values of x_g and y_g. Thus, they could also be absorbed in the scaling factor, redefining

$$\begin{aligned} \xi' &= s\, \xi , \\ \hat{I}' &= s^2\, \hat{I} . \end{aligned} \tag{43}$$

Since $\hat{I}$ is given analytically in terms of the gyrotron parameters, it suffices to compute tables of $\hat{\Gamma}$, $\hat{G}$ and $\hat{D}$ as functions of ν_m once, to completely know the coupling coefficients for any combination of the parameters I, μ, β_{zo}, $\beta_{\perp o}$ and frequencies ω_m. Note that the beam spatial profile enters only in the nonlinear filling factor S_j; in case of complicated beam profiles S_j can be computed independently from Eq. (33). The discussion so far has been limited to a cold beam. In case of thermal effects the general expressions (A7) and (A8) are applicable and the control space will increase by two parameters, the pitch angle spread and the energy spread.

Equations (37) and their reduced form, Eqs. (41), are the basic result in this paper, and describe three mode interaction up to fifth

order in magnitude in the QOG. The diagonal terms G_{nn} describe the effects of nonlinear saturation (or self excitation) for each mode. The cross-coupling terms G_{nm} describe a phase-independe. . nonlinear damping (positive or negative) among different modes. The interaction through the G_{nml} terms does involve the slow phase and describes mode locking effects. The fifth order terms D_{nml} are necessary to stabilize the system in regimes where most of the third order interactions are positive and mutually destabilizing. They are also required to account for potential amplitude bistability,[15] i.e., the existence of two equilibria of the same frequency but of different amplitude.

Similar results, to third order in amplitude, have been obtained for the conventional gyrotron[11], using a somewhat different approach. The present derivation of the coefficients is considerably simpler, since it requires a (j+1)-fold integration for the j-th order, compared to the (2j+1)-fold integration required in the single particle approach.[11] Mode coupling equations, identical in structure, first appeared in the treatment of LASER cavities[16].

VI. RESULTS AND CONCLUSIONS

The normalized linear growth rate $\mathrm{Re}\hat{\Gamma}(\nu_n)$ is given in Fig. 2. Tables of the third order coupling coefficients $\hat{G}(\nu_n, \nu_m)$ for Gaussian profile modes and a cold pencil electron beam have been obtained by numerical evaluation of the expressions (B5)-(B7). The contour plots for the real and imaginary parts of $\hat{G}_{nm}$, $\hat{G}_{123}$ and $\hat{G}_{231}$ within the regime $0 < \nu_n, \nu_m < 3$ are shown in Figs. 3a, 3b, and 3c respectively (the coefficients $\hat{G}_{312}$ are given in terms of $\hat{G}_{123}$, $\hat{G}_{312}(\nu_1, \nu_2) = \hat{G}_{123}(\nu_3, \nu_2)$). Dotted lines represent regions of negative values for $\hat{G}$, corresponding to mutually stabilizing influence among interacting modes in that region. The mode coupling is destabilizing in the regions with solid lines, corresponding to positive $\hat{G}$. Note the absence of symmetry in the coupling coefficients, where, in general, $G_{nm} \neq G_{mn}$. Contour plots for the fifth order coupling coefficients $\hat{D}(\nu_n, \nu_m, \nu_l)$ as functions of ν_m, ν_l for selected values of ν_n appear in Figs. 4(a)-4(d).

According to the final number of participating equilibrium modes, Eqs. (41) demonstrate three types of equilibria: (a) single mode, where one mode dominates the other two (b) two mode equilibria, where one mode is of negligible amplitude and (c) equilibria among three modes of comparable amplitudes. The complete set of equilibria among a given set of frequencies is given by the zeros of the right-hand side of (42). Since F_n are defined positive, only solutions with F_1, F_2, $F_3 > 0$ are acceptable. It is well known that every stable equilibrium of a nonlinear dissipative system, such as the system represented by Eqs. (41), is associated with a region of initial conditions in amplitude space (basin of attraction) that eventually fall into this equilibrium. Which equilibrium the system will choose to settle in cannot be analytically

predicted, in the absence of invariants of the motion. This can only be done by integration of the set of ordinary differential equations (41).

The simplest case, a single mode equilibrium for the n-th mode, is found from

$$\frac{dF_n}{dt} = F_n \left(Re\Gamma_n + ReG_{nn} F_n^2 + ReD_{nnn} F_n^4 \right) = 0 , \qquad (44a)$$

$$\frac{d\phi_n}{dt} = Im\Gamma_n - F_n^2 \left(ImG_{nn} + ImD_{nnn} F_n^2 \right) . \qquad (44b)$$

Equations (44) are obtained by dropping the cross-coupling terms from (37); the combined phase Φ is irrelevant in that case. Acceptable, non-trivial solutions $F_n > 0$ for the steady-state amplitude should always exist, since a single mode saturates through particle trapping. The fifth order saturation term D_{nnn} is therefore important on two counts. First, it is necessary for saturation in regimes where the third order G_{nn} is positive and causes self-excitation instead of suppression. Second, it is required to account for amplitude bistability, when two acceptable equilibrium values F_{n1} and F_{n2} exist for a given mode, since the third order nonzero solutions, $F_n = \pm (\Gamma_n/G_{nn})^{1/2}$, can provide at most one acceptable solution $F > 0$. At steady-state the slow phase ϕ_n varies at a constant rate, Eq. (44b); $d\phi_n/dt$ expresses the nonlinear frequency shift from the linear frequency ω_n.

Equations (37) are used to provide some examples of mode competition in a QOG driven by a cold pencil beam in a typical parameter regime, with beam current $I_b = 13$ A, $\gamma_o = 1.146$, $\beta_{\perp o}/\beta_{zo} = 1$, $W/\lambda = 5$, cavity $Q = 40{,}000$ and cavity length $L = 48$cm, corresponding to a frequency separation $d\omega/\omega_o = 0.003$. In Figs. 4(a)-4(c) we examine mode interaction

among the first three frequencies $\omega_1 < \omega_2 < \omega_3$ above ω_o, counting only the odd resonator modes ω_n separated by $d\omega/\omega_o = 0.006$. In Fig. 5(a) initially $F_{2o} >> F_{1o}, F_{3o}$. The mode F_2 quickly reaches a quasi-steady state, which, however, is unstable. The mode F_3, which initially grows much slowly than its uncoupled linear rate due to nonlinear suppression from F_2, eventually overtakes and suppresses F_2 (mode switching in the cavity). In contrast, the steady state reached from $F_{1o} >> F_{2o}, F_{3o}$, shown in Fig. 5(b), is stable since a large amplitude F_1 suppresses F_2 and F_3 to negligible amplitude. However, the single mode equilibrium of F_1 is not accessible from the usual start-up initial conditions, where all three modes have small comparable amplitudes $F_{1o} \simeq F_{2o} \simeq F_{3o} << 1$. Figure 5(c) shows that the final state in this case has F_3 as the dominant mode. Note that F_2 has been completely suppressed in Fig. 5(c), although its linear growth rate differs from F_2 by a few percent. Since F_3 wins the competition with F_1 and F_2, we next examine the coupling of F_3 with the next two frequencies F_4 and F_5. It is seen from Fig. 6 that the final steady state involves three modes with comparable amplitudes. Note that F_5 has been excited despite being linearly stable. Figure 7 shows the mode competition among the first three modes in a cavity of reduced length, L = 24cm, and increased frequency separation $d\omega/\omega_o = 0.012$ among odd modes.

In conclusion, the general analytic formalism for multimode interaction in the QOG has been developed in this paper. Applications of the coupling equations to interactions involving three main modes have demonstrated the ability to model nonlinear effects, such as nonlinear destabilization, suppression, and mode switching. A new scaling has been introduced, during the derivation of the coupling equations, that reduces the number of the control parameters. The ratio of operation to start-up current $\dot{I}$, and the desynchronism parameters ν_i for the participating modes

become the only free parameters. The inclusion of coupling terms up to fifth order in amplitude was shown to stabilize the system in the hard excitation regime (where the third order coupling coefficients are positive.) The coupling coefficients up to fifth order have been tabulated for a cold pencil beam. These results will be generalized in a future paper to include thermal spreads in velocity, and arbitrary beam current profiles. The set of equations will also be expanded to include interactions among a large number of modes, by forming all the possible resonant frequency combinations.

Acknowledgement

This work supported by the Office of Fusion Energy of the Department of Energy and by the Office of Naval Research.

REFERENCES

1. P. Sprangle, J. L. Vomvorides and W. M. Manheimer, Appl. Phys. Lett. 38 (5), 310 (1981); Phys. Rev. A23, 3127 (1981).
2. J. L. Vomvorides and P.Sprangle, Phys. Rev. A25, 931 (1982).
3. P. Sprangle, C. M. Tang and P. Serafim, Appl. Phys. Lett. 49 (18), 1154 (1986).
4. S. Riyopoulos, P. Sprangle and C. M. Tang, Phys. Rev. A36, 197 (1987).
5. S. Riyopoulos, C. M. Tang, P. Sprangle and B. Levush, Phys. Fluids 31, 924 (1988).
6. V. L. Bratman, N. S. Ginzburg, G. S. Nusinovich, M. I. Petelin and P. S. Strelkov, Int. J. Electron. 51, 541 (1981).
7. B. G. Danly and R. J. Temkin, Phys. Fluids 29, 561 (1986).
8. A. Bondenson, W. M. Manheimer and E. Ott, Infrared and Millimeter Waves, K. J. Button, ed., (Academic Press, New York, 1983), Vol. 9, chapter 7.
9. A. W. Fliflet, T. A. Hargreaves, W. M. Manheimer, R. P. Fischer, M. L. Barsanti, B. Levush and T. M. Antonsen Jr., submitted to Phys. Fluids B (1989).
10. T. M. Antonsen Jr., B. Levush and W. M. Manheimer, submitted to Phys. Fluids B (1989).
11. G. S. Nusinovich, Intl. J. Electron. 51 (4), 457 (1981).
12. A. W. Fliflet and W. M. Manheimer, Phys. Rev. A39, 3432 (1989).
13. W. M. Manheimer, Intl. J. Electron. 63 (1), 29 (1987).
14. See, for example, V. N. Tsytovich in "Nonlinear Effects in Plasmas" (Plenum Press, New York, N.Y. 1970) p. 32.
15. D. Dialetis and K. R. Chu, Infrared and Millimeter Waves, K. J. Button, ed., (Academic Press, New York, 1983), Vol. 7, chapter 10.
16. W. E. Lamp, Phys. Rev. 134, 1429 (1964).

Appendix A: Computation of the Nonlinear Current

Substituting operator (28) inside (27) and performing the successive iterations yields

$$f^{(1)}(u_\perp,\theta,\zeta;t) = \frac{kW}{2i}\sum_n \tilde{a}_n\, e^{i(\psi_n+\nu_n\zeta)} \int_{-\infty}^{\zeta} d\zeta_1\, \chi_{-n}(\zeta_1,u_\perp)\, \frac{\partial f^{(0)}}{\partial u_\perp} + cc\ , \quad (A1)$$

$$f^{(2)}(u_\perp,\theta,\zeta;t) = \left(\frac{kW}{2i}\right)^2 \sum_n \sum_m \tilde{a}_n\, \tilde{a}_m^{*} \Bigg\{$$

$$e^{i(\psi_n-\psi_m)}\, e^{i(\nu_n-\nu_m)\zeta} \int_{-\infty}^{\zeta} d\zeta_1\, \chi_{-n}\, \frac{\partial}{\partial u_\perp} \int_{-\infty}^{\zeta_1} d\zeta_2\, \chi_m$$

$$+ \left[\, n,\ m \,\right]$$

$$+ e^{i(\psi_n-\psi_m)}\, e^{i(\nu_n-\nu_m)\zeta} \int_{-\infty}^{\zeta} d\zeta_1\, \chi_{-n}\, \frac{1}{u_\perp} \int_{-\infty}^{\zeta_1} d\zeta_2\, \chi_m$$

$$+ \left[\, n,\ m \,\right] \Bigg\} \frac{\partial f^{(0)}}{\partial u_\perp} + cc\ , \quad (A2)$$

and

$$f^{(3)}(u_\perp,\theta,\zeta,t) = \left(\frac{kW}{2i}\right)^3 \sum_n \sum_m \sum_l \tilde{a}_n \tilde{a}_m^* \tilde{a}_l^* \Bigg\{$$

$$e^{i(\psi_n - \psi_m - \psi_l)}\, e^{i(\nu_n - \nu_m - \nu_l)\zeta} \int_{-\infty}^{\zeta} d\zeta_1\, \chi_{-n} \frac{\partial}{\partial u_\perp} \int_{-\infty}^{\zeta_1} d\zeta_2\, \chi_m \frac{\partial}{\partial u_\perp} \int_{-\infty}^{\zeta_2} d\zeta_3\, \chi_l$$

$$+ \left[-n,\ m,\ -l \right] + \left[-n,\ -m,\ l \right] + \left[-n,\ -m,\ -l \right] +$$

$$e^{i(\psi_n - \psi_m - \psi_l)}\, e^{i(\nu_n - \nu_m - \nu_l)\zeta} \int_{-\infty}^{\zeta} d\zeta_1\, \chi_{-n} \frac{\partial}{\partial u_\perp} \int_{-\infty}^{\zeta_1} d\zeta_2\, \chi_{-m} \frac{1}{u_\perp} \int_{-\infty}^{\zeta_2} d\zeta_3\, \dot{\chi}_l$$

$$+ \left[-n,\ m,\ -l \right] + \left[-n,\ -m,\ l \right] + \left[-n,\ -m,\ -l \right] +$$

$$e^{i(\psi_n - \psi_m - \psi_l)}\, e^{i(\nu_n - \nu_m - \nu_l)\zeta} \int_{-\infty}^{\zeta} d\zeta_1\, \chi_{-n} \frac{1}{u_\perp} \int_{-\infty}^{\zeta_1} d\zeta_2\, \dot{\chi}_m \frac{\partial}{\partial u_\perp} \int_{-\infty}^{\zeta_2} d\zeta_3\, \chi_l$$

$$+ \left[-n,\ -m,\ -l \right]$$

$$e^{i(\psi_n - \psi_m - \psi_l)}\, e^{i(\nu_n - \nu_m - \nu_l)\zeta} \int_{-\infty}^{\zeta} d\zeta_1\, \chi_{-n} \frac{1}{u_\perp} \int_{-\infty}^{\zeta_1} d\zeta_2\, \dot{\chi}_m \frac{1}{u_\perp} \int_{-\infty}^{\zeta_2} d\zeta_3\, \dot{\chi}_l$$

$$+ \left[-n,\ -m,\ -l \right] \Bigg\} \frac{\partial f^{(0)}}{\partial u_\perp} + cc\ , \qquad \text{(A3)}$$

where the explicit θ, t dependence is contained in $\psi_n = \theta - \omega_n t$,

$$\chi_n(\zeta,u_\perp) = \frac{\gamma}{u_{zo}} J_1'\left(\frac{k_n u_\perp}{\Omega_o}\right) \cos k_n x_g\, h_n(\zeta)\, e^{i\nu_n\zeta}\ , \qquad \chi_{-n}(\zeta,u_\perp) \equiv \chi_n(\zeta,u_\perp)^*\ ,$$

$$\dot{\chi}_n(\zeta,u_\perp) = \chi_n(\zeta,u_\perp)\, J_1\left(\frac{k_n u_\perp}{\Omega_o}\right) / J_1'\left(\frac{k_n u_\perp}{\Omega_o}\right) \left(\frac{k_n u_\perp}{\Omega_o}\right)\ , \qquad \dot{\chi}_{-n}(\zeta,u_\perp) \equiv \dot{\chi}_n(\zeta,u_\perp)^*\ .$$

In obtaining (A1)-(A3) we used the invariance: $\psi_n + \nu_n\zeta = \text{const.}$, along the unperturbed trajectories. The notation [-n, m, -l] inside (A2)-(A3)

means an integral similar to the preceding fully written term except that a negative index -n in place of n implies $-\psi_n$, $-\nu_n$, $\chi_n \tilde{a}_n^*$ in place of ψ_n, ν_n, χ_{-n}, $\tilde{a}_n$, etc.

The dominant contribution in each integral comes from the derivative $\partial/\partial u_\perp$ acting on ν_m,

$$\frac{\partial \nu_m}{\partial u_\perp} = \frac{\omega_m}{\omega_o}\,\eta(u_\perp), \quad \text{where} \quad \eta(u_\perp) = \frac{k_o W u_\perp}{\gamma\, u_z} = \frac{2\pi W}{\lambda\gamma}\,\frac{u_\perp}{u_z} >> 1 \,. \tag{A4}$$

Therefore, the most important terms inside $f^{(j)}$ are those with the $(\partial/\partial u_\perp)^j$ derivative. Neglecting, for the same reason, terms like $\partial\gamma/\partial u_\perp \sim \partial u_\perp^{\,k}/\partial u_\perp \sim 1 << \partial\nu_m/\partial u_\perp$ one obtains from (A3)

$$f^{(3)}(u_\perp,\theta,\zeta,t) = \left(\frac{kW}{2i}\right)^3 \left(\frac{\gamma}{u_{zo}}\right)^3 \sum_n \sum_m \sum_l s_n\, s_m\, s_l\, \tilde{a}_n\, \tilde{a}_m^*\, \tilde{a}_l^*$$

$$e^{i(\psi_n - \psi_m - \psi_l)}\; e^{i(\nu_n - \nu_m - \nu_l)\zeta} \int_{-\infty}^{\zeta} d\zeta_1\; v_{-n}\, \frac{\partial}{\partial u_\perp} \int_{-\infty}^{\zeta_1} d\zeta_2\; v_m\, \frac{\partial}{\partial u_\perp} \int_{-\infty}^{\zeta_2} d\zeta_3\; v_l\, \frac{\partial f^{(0)}}{\partial u_\perp}$$

$$+ \left[-n, m, -l\right] + \left[-n, -m, l\right] + \left[-n, -m, -l\right] + cc \,, \tag{A5}$$

where $v_m(\zeta) = J_1'\left(\frac{k_n u_\perp}{\varrho_o}\right) h_m(\zeta)\, e^{i\nu_m\zeta}$, $\quad s_m = \cos k_m x_g\; h_m(y_g)$.

One can show by induction, proceeding along the same lines, that

$$f^{(j)}(u_\perp,\theta,\zeta,t) = \left(\frac{kW}{2i}\right)^j \left(\frac{\gamma}{u_{zo}}\right)^j \sum_{m_1}\sum_{m_2}\cdots\sum_{m_j} s_{m_1} s_{m_2}\cdots s_{m_j}\, \tilde{a}_{m_1}\tilde{a}^*_{m_2}\tilde{a}_{m_3}\cdots\tilde{a}^*_{m_j}$$

$$e^{i(\psi_{m_1}-\psi_{m_2}+\psi_{m_3}-\cdots-\psi_{m_j})}\; e^{i(\nu_{m_1}-\nu_{m_2}+\nu_{m_3}-\cdots-\nu_{m_j})\zeta}$$

$$\int_{-\infty}^{\zeta} d\zeta_1\, \nu_{-m_1} \frac{\partial}{\partial u_\perp}\int_{-\infty}^{\zeta_1} d\zeta_2\, \nu_{m_2} \frac{\partial}{\partial u_\perp}\int_{-\infty}^{\zeta_2} d\zeta_3\, \nu_{-m_3}\cdots \frac{\partial}{\partial u_\perp}\int_{-\infty}^{\zeta_{j-1}} d\zeta_j\, \nu_{m_j} \frac{\partial f^{(0)}}{\partial u_\perp}$$

$$+ \left\{ m_1, -m_2, m_3, \cdots, -m_j \right\} + cc\,, \qquad (A6)$$

where { ... } implies all the permutations among the m_j' s.

When the j-th nonlinear piece $f^{(j)}$ of f_{NL} is substituted inside (15) and combined with $\cos\theta = (1/2)(e^{i\theta} + e^{-i\theta})$, the resulting expression contains even θ-harmonics, 1, $e^{\pm 2i\theta}$, ..., $e^{\pm(j+1)i\theta}$, for j odd, and odd θ-harmonics, $e^{\pm i\theta}$, $e^{\pm 3i\theta}$, ..., $e^{\pm(j+1)i\theta}$, for j even. Consequently, coupling interactions involving even number of modes vanish completely during the θ-integration. The first nonlinear correction is of third order in amplitude, the second of fifth, and so on. It should be emphasized that this is a consequence of assuming a uniform in θ initial distribution $f^{(0)}(u)$; however, for a prebunched distribution of the form $f^{(0)}(u,\theta) = \tilde{f}_o(u) + \tilde{f}_1(u)\, e^{i\theta} + \ldots + cc$, both even and odd terms survive and the nonlinear effects enter to second order in amplitude. Splitting the slowly varying $f_{NL}(\omega_n)$ component off the nonlinear distribution, by multiplying each $f^{(j)}$ with $\exp(i\omega_n t)$ and averaging over the fast time, substituting $f_{NL}(\omega_n)$ inside (19), and finally averaging over the gyroangle θ and over the resonator volume, one obtains

$$\langle j_{NL}(\omega_n)\rangle = \frac{I_o}{\sigma_b V_n}\frac{\gamma_o}{u_{zo}} \sum_{\{m_1,m_2,m_3,\ldots,m_j;n\}}$$

$$\left(C^{(1)}_{m_1;n}\,\tilde{a}_{m_j} + C^{(3)}_{m_1,m_2,m_3;n}\,\tilde{a}_{m_1}\,\tilde{a}_{m_2}\,\tilde{a}_{m_3} + \ldots + C^{(j)}_{m_1,m_2,m_3,\ldots,m_j;n}\,\tilde{a}_{m_1}\,\tilde{a}_{m_2}\ldots\tilde{a}_{m_j}\right), \tag{A7}$$

$$C^{(j)}_{m_1\ldots m_j;n} = \left(\frac{i}{2}\right)^j (kW)^{j+1} S_{m_1\ldots m_j;n}\,\exp\left[i\left(\Delta\omega_{m_1\ldots m_j;n}t + \Phi_{m_1\ldots m_j;n}\right)\right]\int_0^\infty du_\perp \frac{u_\perp^2}{\gamma}\left(\frac{\gamma}{u_{zo}}\right)^j$$

$$\int_{-\infty}^{\infty} dz\; v_n(z)\int_{-\infty}^{z} d\zeta_1\; v_{m_1}(\zeta_1)\,\frac{\partial}{\partial u_\perp}\int_{-\infty}^{\zeta_1} d\zeta_2\; v_{m_2}(\zeta_2)\,\frac{\partial}{\partial u_\perp}\int_{-\infty}^{\zeta_2}\ldots\,\frac{\partial}{\partial u_\perp}\int_{-\infty}^{\zeta_{j-1}} d\zeta_j v_{m_j}(\zeta_j)\,\frac{df^{(0)}}{du_\perp}\;. \tag{A8}$$

The quantities $\Delta\omega_{m_1m_2\ldots m_j;n}$, v_{m_j}, $\Phi_{m_1m_2\ldots m_j;n}$ and $S_{m_1m_2\ldots m_j;n}$ are defined in a similar manner as in equations (30), (32) and (33) respectively. Of all the possible combinations $[m_1\pm m_2\pm m_3\pm\ldots\pm m_j]$ only those with (j-1)/2 positive and (j+1)/2 negative signs have survived the θ-integration and contribute to $C^{(j)}$; for example, the term [-l,-m,-n] in $f^{(3)}$, Eq. (A5), has vanished from $C^{(3)}$. Also note that the complex conjugate terms in (A1)-(A6) drop out during the fast time averaging; they contribute to the $j_{NL}(-\omega_n)$ component.

Appendix B: Computation of the Three-Mode Coupling Coefficients

The three-mode coupling coefficients in Eqs. (37) are computed from the general expressions in (31), keeping the frequency combinations (35) and (36), and yielding,

$$\Gamma_n = K\, C^{(1)}_{-n;n}, \quad G_{nm} = K \sum_{\{-m,m,-n\}} C^{(3)}_{-mm-n;n},$$

$$G_{123} = K \sum_{\{-2,-2,3\}} C^{(3)}_{-2-23;1}, \quad G_{312} = K \sum_{\{-2,-2,1\}} C^{(3)}_{-2-21;3}, \quad G_{231} = K \sum_{\{2,-3,-1\}} C^{(3)}_{2-3-1;2} .$$

$$D_{m123} = K \sum_{\{-m,m,-2,-2,3\}} C^{(5)}_{-mm-2-23;1}, \qquad D_{nlm} = K \sum_{\{-m,m,-1,1,-n\}} C^{(5)}_{-mm-11-n;n},$$

$$\text{where } K = 2\pi i \frac{\gamma_o}{u_{zo}} \frac{I}{\sigma_b V} . \tag{B1}$$

A cold pencil beam is employed for simplicity, where the velocity distribution $f^{(0)}$ and the density profile $\hat{n}(x_g,y_g)$ are given by

$$f^{(0)} = \frac{1}{2\pi u_{\perp o}} \delta(u_\perp - u_{\perp o})\, \delta(u_z - u_{zo}) , \qquad \hat{n}(x_g,y_g) = \delta(x_g - \tfrac{L}{2})\, \delta(y_g) .$$

The calculations are simplified by the following observation involving the derivatives of $\delta(u_\perp - u_{\perp o})$. If A(u), B(u) are any functions of u satisfying $d^nA/du^n \ll d^nB/du^n$ for every n, then

$$\int du\, A\, B\, \frac{d\delta}{du} = - \int du \left(\frac{dA}{du} B + \frac{dB}{du} A\right) \delta \simeq - A \frac{dB}{du}\Big|_{u_o} = A(u_o) \int du\, B\, \frac{d\delta}{du} ,$$

and by induction

$$\int du\ A\ B\ \frac{d^n\delta}{du^n} = A(u_o) \int du\ B\ \frac{d^n\delta}{du^n}\ .$$

One can see that $\frac{d^n}{du_\perp^n}\left(\gamma,\ u_\perp^k,\ J(k_n\rho)\right) << \left|\frac{d^n}{du_\perp^n} e^{i\nu_n\zeta}\right| \sim \eta_o^n$, where

$$\eta_o \equiv \eta(u_{\perp o}) = \frac{k_o W}{\gamma_o}\frac{\beta_{\perp o}}{\beta_{zo}} = \frac{2\mu}{\gamma_o\beta_{\perp o}} >> 1\ . \tag{B2}$$

Therefore, moving everything but the exponentials $\exp(i\nu_n\zeta)$ in front of the velocity integrals, one obtains

$$\Gamma_n = \frac{1}{2}\frac{2\pi I_o}{\sigma_b V_n}\frac{u_{\perp o}}{u_{zo}}\left(\frac{\gamma_o}{u_{zo}}\right)\left(k_o W\right)^2 J_{no}^{\ 2}\ S_1\ \tilde{\Gamma}_n\ , \tag{B3}$$

$$G_{nm} = -\left(\frac{1}{2}\right)^3\frac{2\pi I_o}{\sigma_b V_n}\frac{u_{\perp o}}{u_{zo}}\left(\frac{\gamma_o}{u_{zo}}\right)^3\left(k_o W\right)^4 (J_{no}J_{mo})^2\ S_3\ \tilde{G}_{nm} \tag{B4}$$

$$D_{nlm} = \left(\frac{1}{2}\right)^5\frac{2\pi I_o}{\sigma_b V_n}\frac{u_{\perp o}}{u_{zo}}\left(\frac{\gamma_o}{u_{zo}}\right)^5\left(k_o W\right)^6 (J_{no}J_{lo}J_{mo})^2\ S_5\ \tilde{D}_{nlm}\ , \tag{B5}$$

where $J_{no} \equiv J_1'(k_n\rho_o)$, $\rho_o = u_{\perp o}/\Omega_o$ and

$$\tilde{\Gamma}_n = \int_0^\infty du_\perp \int_{-\infty}^{\infty} d\zeta\ \dot{v}_n \int_{-\infty}^{\zeta} d\zeta_1\ \dot{v}_{-n}\frac{\partial}{\partial u_\perp}\delta\left(u_\perp - u_{\perp o}\right)\ , \tag{B6}$$

$$\tilde{G}_{nm} = \sum_{\{-n,m,-m\}} \int_0^\infty du_\perp \int_{-\infty}^{\infty} d\zeta\ \dot{v}_n \int_{-\infty}^{\zeta} d\zeta_1\ \dot{v}_{-n}\frac{\partial}{\partial u_\perp}\int_{-\infty}^{\zeta_1} d\zeta_2\ \dot{v}_m\frac{\partial}{\partial u_\perp}\int_{-\infty}^{\zeta_2} d\zeta_3\ \dot{v}_{-m}$$

$$\times\frac{\partial}{\partial u_\perp}\delta\left(u_\perp - u_{\perp o}\right)\ , \tag{B7}$$

$$\tilde{D}_{nlm} = \sum_{\{n,-l,l,-m,m\}} \int_0^\infty du_\perp \int_{-\infty}^{\infty} d\zeta\, \dot{v}_n \int_{-\infty}^{\zeta} d\zeta_1\, \dot{v}_{-n} \frac{\partial}{\partial u_\perp} \int_{-\infty}^{\zeta_1} d\zeta_2\, \dot{v}_1 \frac{\partial}{\partial u_\perp} \int_{-\infty}^{\zeta_2} d\zeta_3\, \dot{v}_{-1}$$

$$\frac{\partial}{\partial u_\perp} \int_{-\infty}^{\zeta_3} d\zeta_4\, \dot{v}_m \frac{\partial}{\partial u_\perp} \int_{-\infty}^{\zeta_4} d\zeta_5\, \dot{v}_{-m} \frac{\partial}{\partial u_\perp} \delta\left(u_\perp - u_{\perp o}\right) , \qquad \text{(B8)}$$

where

$$\dot{v}_n(\zeta) = e^{i\nu_n \zeta}\, h_n(\zeta) \quad .$$

We limit the mode coupling among fundamental Gaussian modes where the transverse profiles u_{00} are

$$u_{00}(y_g, z) = h_0(y_g)\, h_0(z) , \qquad h_0(z) = \exp\left(-\frac{z^2}{W^2}\right) , \qquad \text{(B9)}$$

for all frequencies ω_n. The normalized volume in that case is given by

$$V_n = 2\int_0^{\frac{L}{2}} dx \int_{-\infty}^{\infty} dy \int_{-\infty}^{\infty} dz\, \frac{\cos^2 k_n x}{\left(1 + \frac{x^2}{b_n^2}\right)^{1/2}} \exp\left(-2\frac{y^2+z^2}{w(x)^2}\right) = \frac{\pi}{2} k_n k_o^2 L\, W^2, \qquad \text{(B10)}$$

$\sigma_b = 1$ and $\dot{v}_n = e^{-\zeta^2}\, e^{i\nu_n \zeta}$.

For the pencil beam at $x_g = L/2$, and according to Eq. (4), $\cos k_n x_g = 0$ for n even and $\cos k_n x_g = 1$ for n odd. In other words, the electron beam passes through a null of the electric field for modes with an even number of half wavelengths between the mirrors, or through a maximum, for an odd number of half wavelengths. The j-th order nonlinear filling factor S_j, Eq. (33), is

then reduced to

$$S_j \equiv S_{m_1 m_2 \ldots m_j;n} = 2\int_0^{L/2} dx_g \int_{-\infty}^{\infty} dy_g\, \hat{n}(x_g,y_g) \left(1 + \frac{x_g^2}{b_o^2}\right)^{-\frac{j+1}{2}} e^{-\frac{(j+1)y_g^2}{W^2}} . \quad (B11)$$

Since the frequency separation among the coupled frequencies ω_n is very small, it is important only when the detuning $\delta\omega_n$, ν_n appears explicitly. Thus, one may set $k_n \simeq k_o$, letting $J_1'(k_n\rho) \simeq J_1'(k_o\rho) \equiv J_o$, $V_n \simeq V = (\pi/2)k_o^3 LW^2$ and $Q_n = Q$ for all modes. To further simplify (B6)-(B10), one may notice that, according to (A4) and for $\omega_n \simeq \omega_o$,

$$\frac{d\nu_n}{du_\perp} \simeq \eta(u_\perp) = \frac{kW}{\gamma}\frac{u_\perp}{u_z}$$

is independent of frequency. Since the δ-function causes every derivative to be taken at $u_\perp = u_{\perp o}$, one may employ ν_n, ν_m, ν_l as independent variables and use

$$\frac{\partial}{\partial u_\perp} = \eta_o\left(\frac{\partial}{\partial \nu_n} + \frac{\partial}{\partial \nu_m} + \frac{\partial}{\partial \nu_l}\right) \equiv \hat{M} , \quad (B12)$$

to show that

$$\tilde{\Gamma}_n = \eta_o\, \hat{\Gamma}(\nu_n) , \quad (B13)$$

$$\tilde{G}_{nm} = \eta_o^3\, \hat{G}(\nu_n,\nu_m) , \quad (B14)$$

$$\tilde{D}_{nlm} = \eta_o^5\, \hat{D}(\nu_n,\nu_l,\nu_m) , \quad (B15)$$

where

$$\hat{\Gamma}(\nu_n) = \int_{-\infty}^{\infty} d\nu_n \int_{-\infty}^{\infty} d\zeta\, \hat{v}_n \int_{-\infty}^{\zeta} d\zeta_1\, \hat{v}_{-n}\, \hat{M}\, \delta\left(\nu_n - \nu_{no}\right) = \frac{\partial}{\partial \nu_{no}} \frac{\pi}{2} e^{-\frac{\nu_{no}^2}{2}}$$

$$= \frac{\pi}{2} \nu_{no} e^{-\frac{\nu_{no}^2}{2}}, \tag{B16}$$

$$\hat{G}(\nu_n, \nu_m) = \sum_{\{-n,m,-m\}} \int_{-\infty}^{\infty}\int_{-\infty}^{\infty} d\nu_n d\nu_m \int_{-\infty}^{\infty} d\zeta\, \hat{v}_n \int_{-\infty}^{\zeta} d\zeta_1\, \hat{v}_{-n}\, \hat{M} \int_{-\infty}^{\zeta_1} d\zeta_2\, \hat{v}_m\, \hat{M} \int_{-\infty}^{\zeta_2} d\zeta_3\, \hat{v}_{-m}$$

$$\hat{M}\, \delta\left(\nu_n - \nu_{no}\right)\, \delta\left(\nu_m - \nu_{mo}\right), \tag{B17}$$

$$\hat{D}(\nu_n, \nu_1, \nu_m) =$$

$$\sum_{\{n,-1,1,-m,m\}} \int_{-\infty}^{\infty}\int_{-\infty}^{\infty}\int_{-\infty}^{\infty} d\nu_n d\nu_1 d\nu_m \int_{-\infty}^{\infty} d\zeta\, \hat{v}_n \int_{-\infty}^{\zeta} d\zeta_1\, \hat{v}_{-n} \hat{M} \int_{-\infty}^{\zeta_1} d\zeta_2\, \hat{v}_1\, \hat{M} \int_{-\infty}^{\zeta_2} d\zeta_3\, \hat{v}_{-1}$$

$$\hat{M} \int_{-\infty}^{\zeta_3} d\zeta_4\, \hat{v}_m\, \hat{M} \int_{-\infty}^{\zeta_4} d\zeta_5\, \hat{v}_{-m}\, \hat{M}\, \delta\left(\nu_1 - \nu_{1o}\right)\, \delta\left(\nu_n - \nu_{no}\right)\, \delta\left(\nu_m - \nu_{mo}\right). \tag{B18}$$

It is clear from (B16)-(B18) that $\hat{\Gamma}$, $\hat{G}$ and $\hat{D}$ depend only on the initial values for the detuning parameters ν_{no}. Combining (B13)-(B15) with (B16)-(B18), converting the amplitudes a_n into the normalized F_n, $a_n = F_n (\gamma_o \beta_{\perp o}{}^3)$, and absorbing the factors $(\gamma_o \beta_{\perp o}{}^3)$ in the coupling coefficients, finally yields

$$\Gamma_n = \frac{2\pi I_o}{\sigma_b V_n} \frac{\beta_{\perp o}}{\beta_{zo}} \left(\frac{1}{2\beta_{zo}}\right) \eta_o \, (k_o W)^2 \, J_o^{\,2} \, S_1 \, \hat{\Gamma}(\nu_n) \tag{B19}$$

$$G_{nm} = \frac{2\pi I_o}{\sigma_b V_n} \frac{\beta_{\perp o}}{\beta_{zo}} \left(\frac{1}{2\beta_{zo}}\right)^3 \left(\gamma_o \beta_{\perp o}^{\,3}\right)^2 \eta_o^{\,3} \, (k_o W)^4 \, J_o^{\,4} \, S_3 \, \hat{G}(\nu_n, \nu_m) \, , \tag{B20}$$

$$D_{nlm} = \frac{2\pi I_o}{\sigma_b V_n} \frac{\beta_{\perp o}}{\beta_{zo}} \left(\frac{1}{2\beta_{zo}}\right)^5 \left(\gamma_o \beta_{\perp o}^{\,3}\right)^4 \eta_o^{\,5} \, (k_o W)^6 \, J_o^{\,6} \, S_5 \, \hat{D}(\nu_n, \nu_l, \nu_m) \, , \tag{B21}$$

and, in general, for the j-th order coupling coefficient,

$$D_{m_1 \ldots m_j} = \frac{2\pi I_o}{\sigma_b V_n} \frac{\beta_{\perp o}}{\beta_{zo}} \left(\frac{1}{2\beta_{zo}}\right)^j \left(\gamma_o \beta_{\perp o}^{\,3}\right)^{j-1} \eta_o^{\,j} \, (k_o W)^{j+1} \, J_o^{\,j+1} \, S_j \, \hat{D}(\nu_{m_1}, \ldots, \nu_{m_j}) \tag{B22}$$

Defining the scaling factor

$$\xi = \frac{\gamma_o \beta_{\perp o}^{\,3}}{2\beta_{zo}} \, k_o W \, J_1'(k_o \rho_o) \, \eta_o \, , \tag{B23}$$

and the new normalized current

$$I_s = \frac{\pi I_o}{V_o} \frac{\beta_{\perp o}^{\,2}}{\gamma_o \beta_{zo}^{\,3}} \, (k_o W)^3 \, [J_1'(k_o \rho_o)]^2 = \frac{I}{8 \, Q_o} \frac{\beta_{\perp o}^{\,5}}{\beta_{zo}^{\,3}} \, [J_1'(k_o \rho_o)]^2 \, (k_o W)^3 , \tag{B24}$$

puts Eqs. (B19)-(B21) in the form given in Eq. (38).

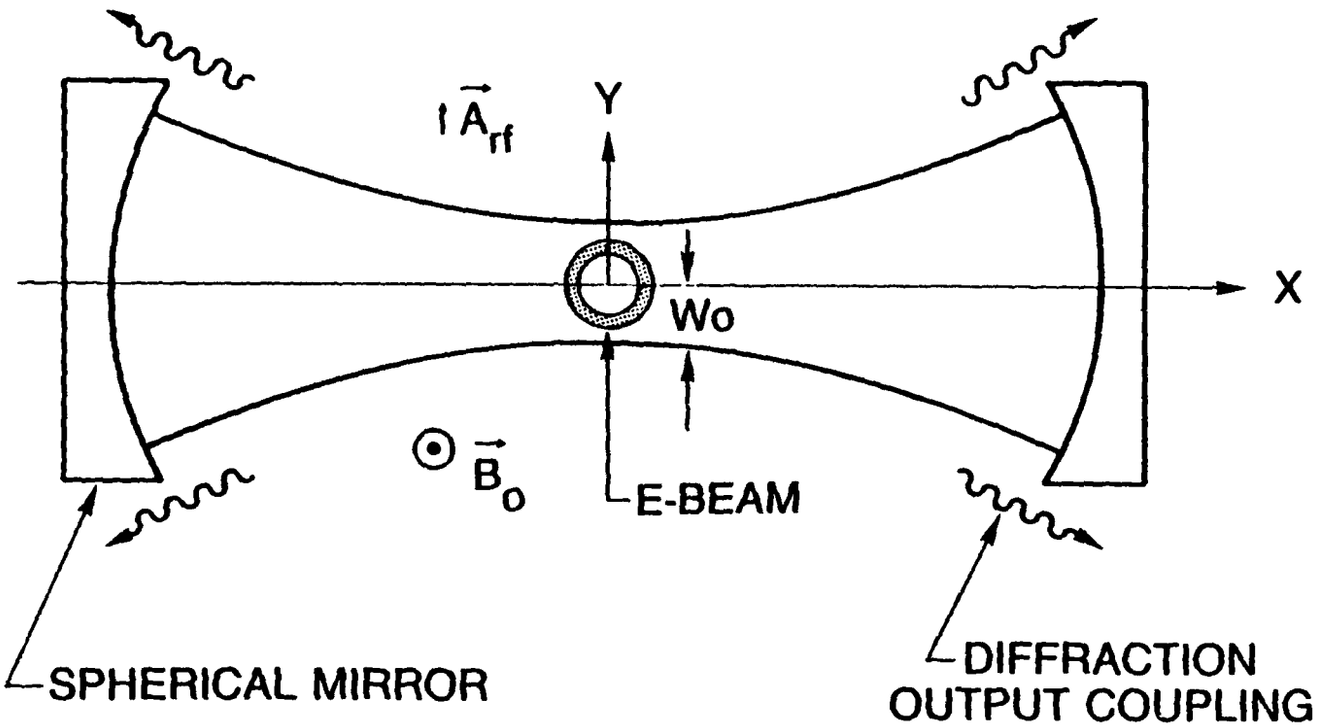

Fig. 1 — Schematic representation of the quasi-optical gyrotron resonator

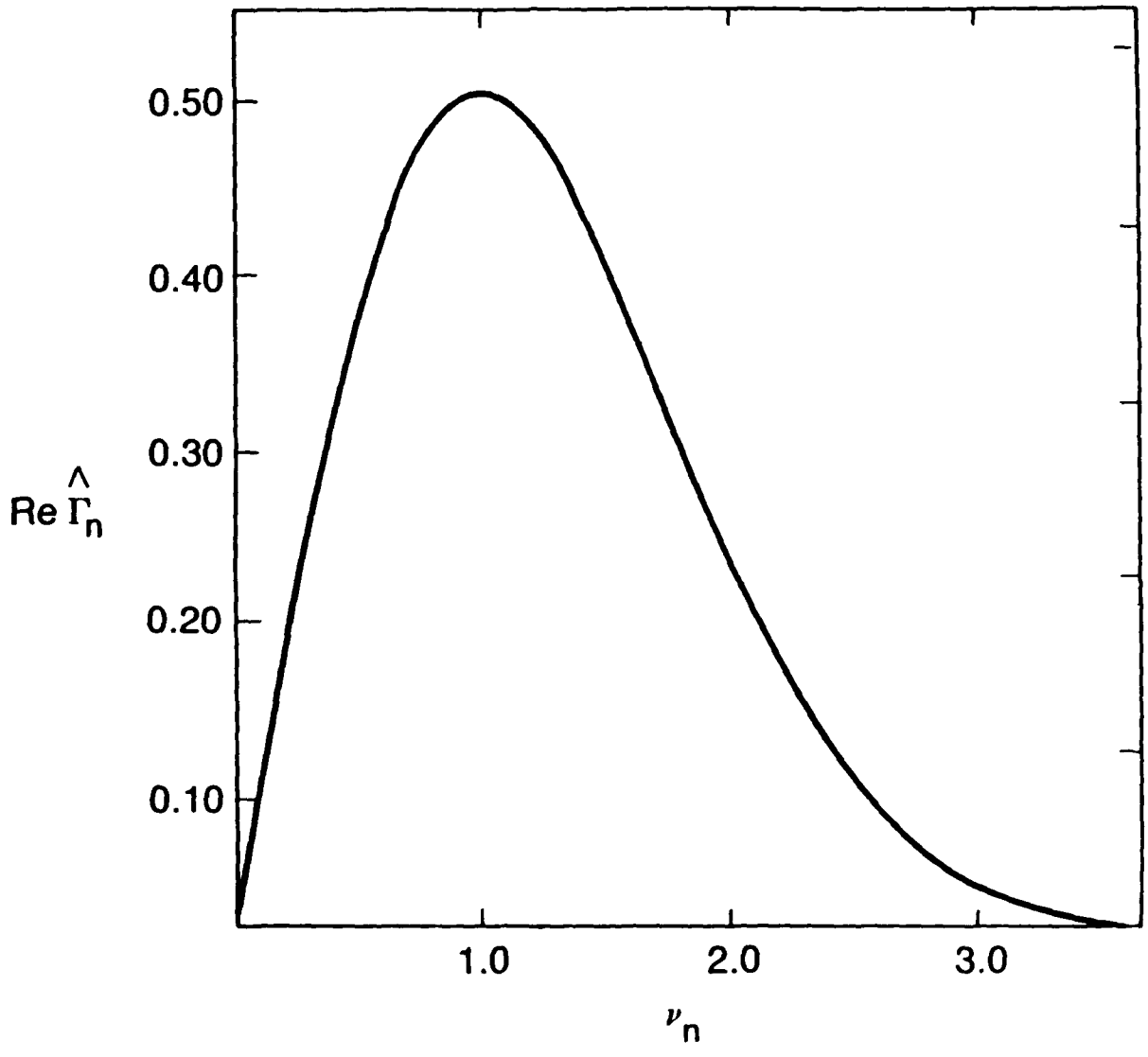

Fig. 2 — Plot of the linear growth rate Γ_n against the mismatch $\delta\omega_n/\omega_o$.

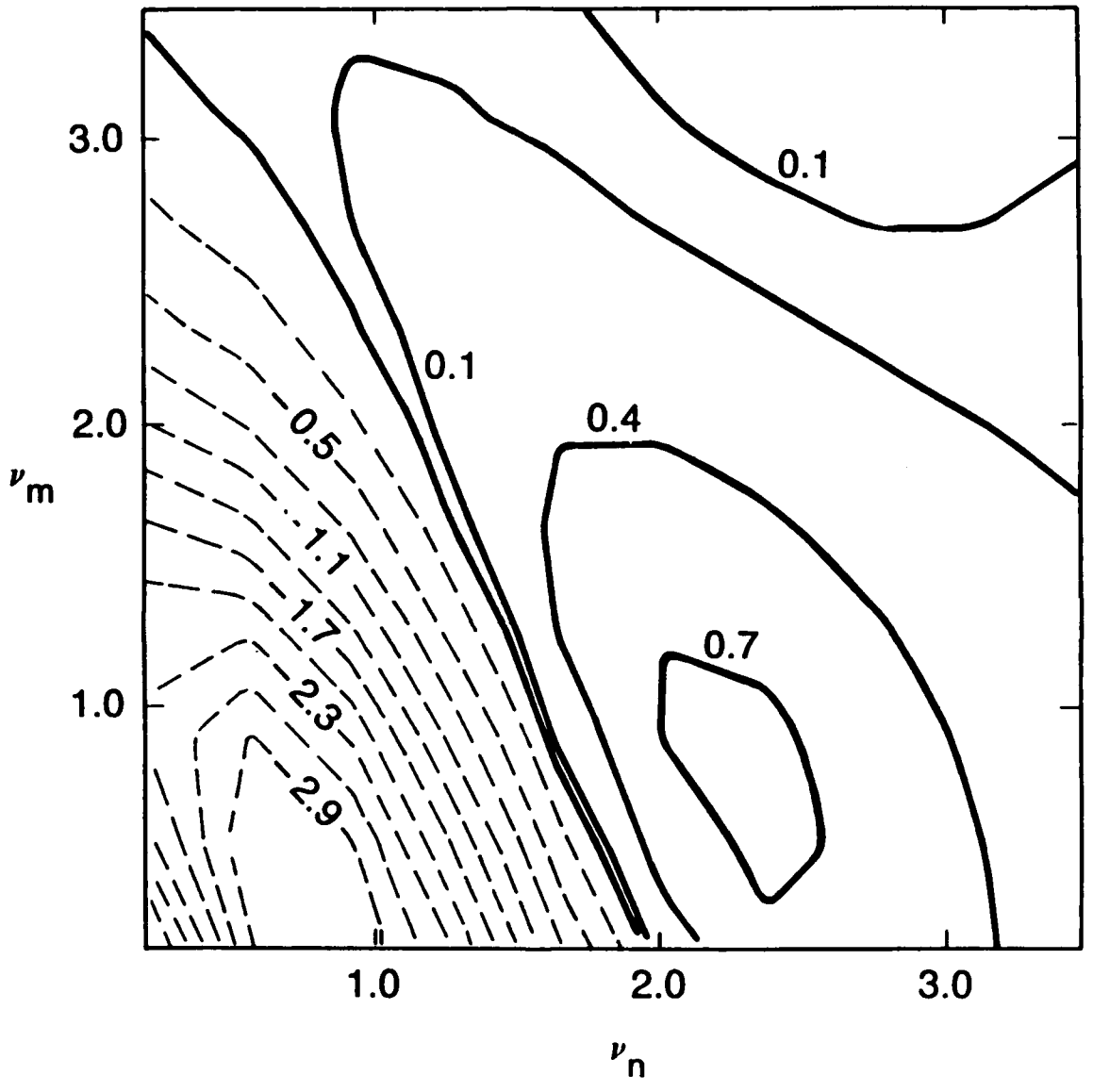

(a)

Fig. 3 — Contour plots for the real parts of third order coupling coefficients (a) $\hat{G}_{mn}$ (b) $\hat{G}_{123}$ and (c) $\hat{G}_{231}$. Dashed lines signify negative values.

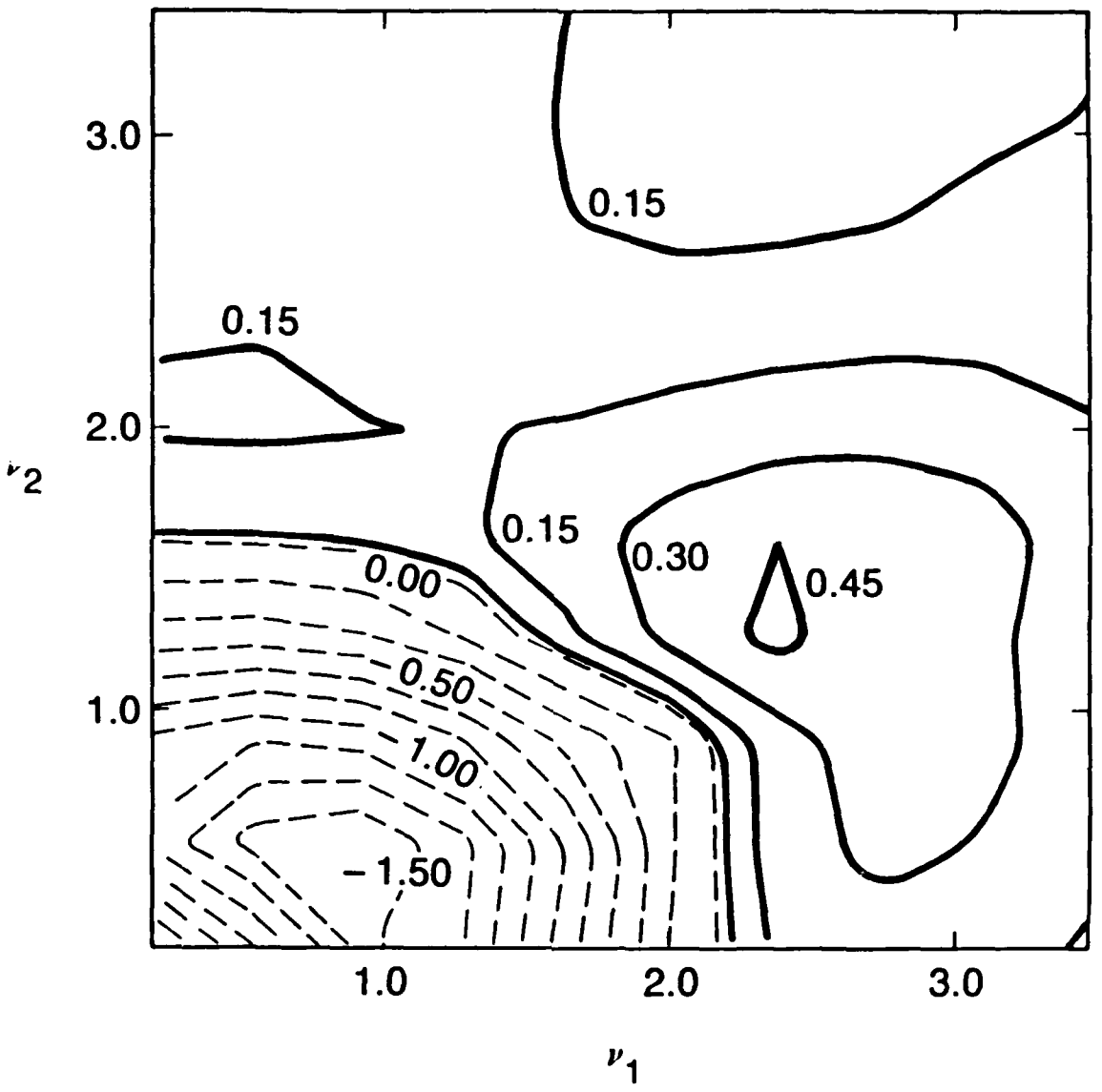

(b)

Fig. 3 (Continued) — Contour plots for the real parts of third order coupling coefficients (a) $\hat{G}_{am}$ (b) $\hat{G}_{123}$ and (c) $\hat{G}_{231}$. Dashed lines signify negative values.

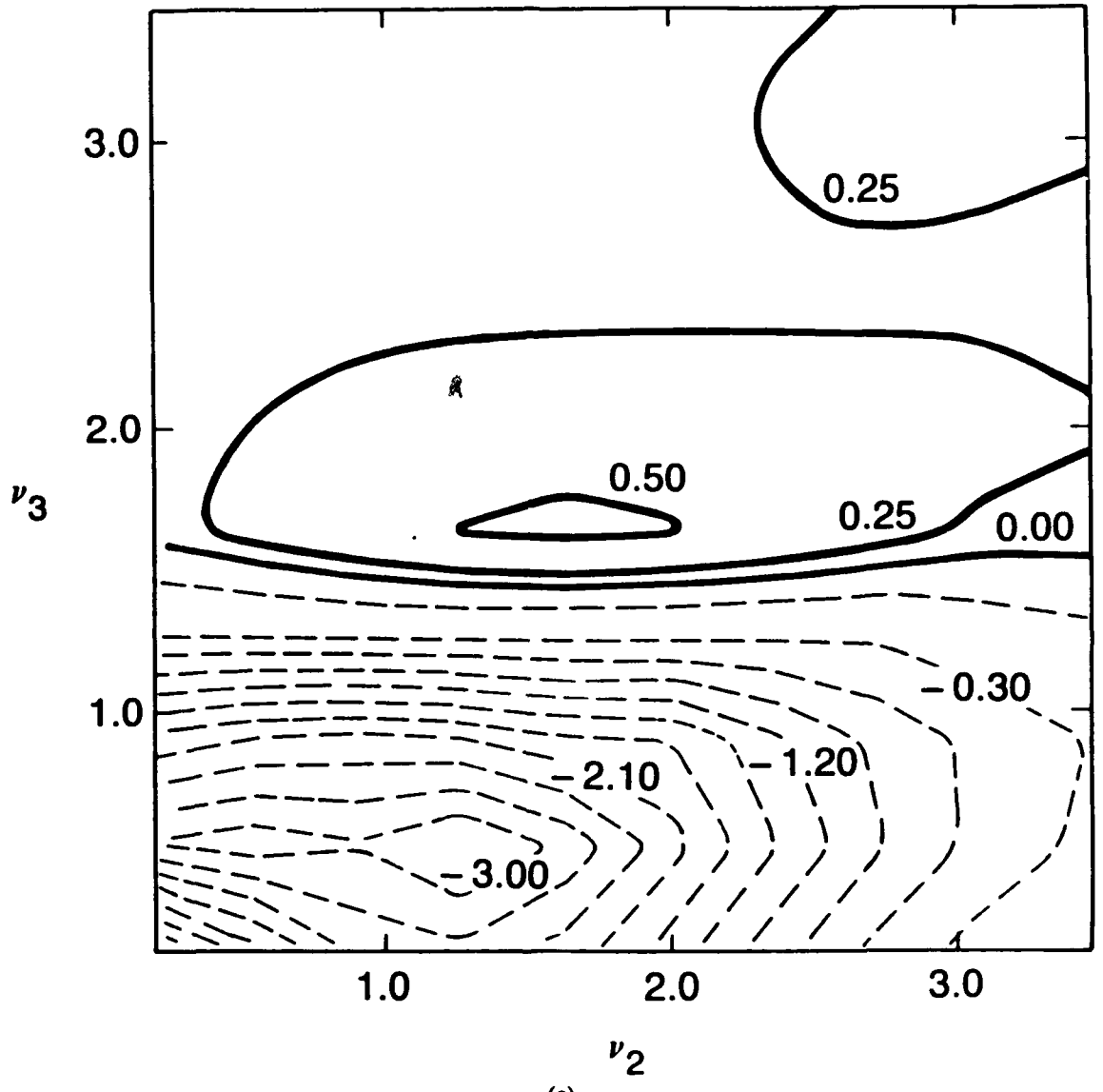

(c)

Fig. 3 (Continued) — Contour plots for the real parts of third order coupling coefficients (a) $\hat{G}_{nn}$ (b) $\hat{G}_{123}$ and (c) $\hat{G}_{231}$. Dashed lines signify negative values.

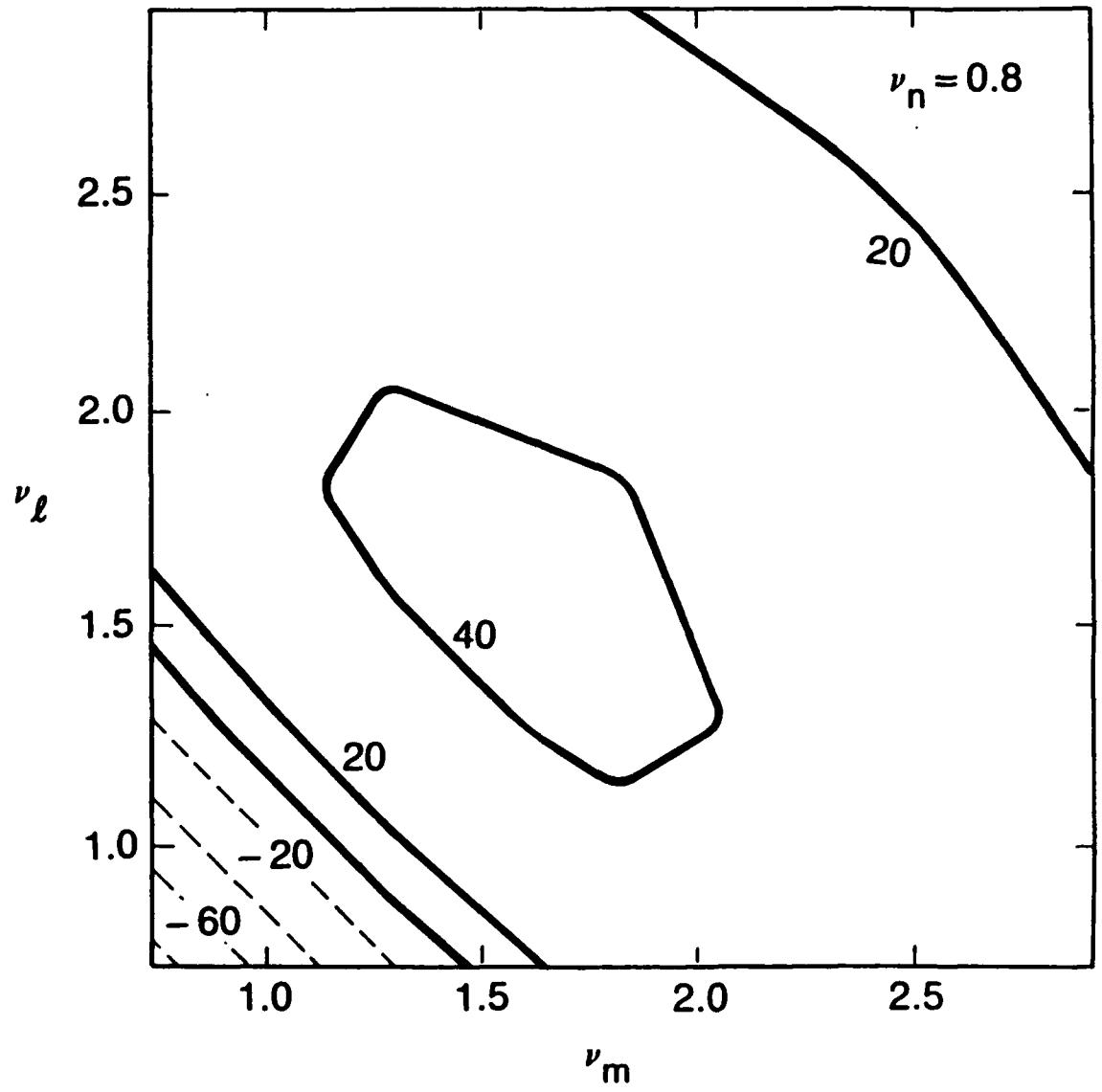

(a)

Fig. 4 — Contour plots for the real parts of the fifth order coupling coefficients $\hat{D}_{nlm}$ on the ν_n = const. plane for (a) $\nu_n = 0.8$ (b) $\nu_n = 1.9$ (c) $\nu_n = 2.9$. The contour plots in (d) are drawn for $\nu_m = \nu_l$.

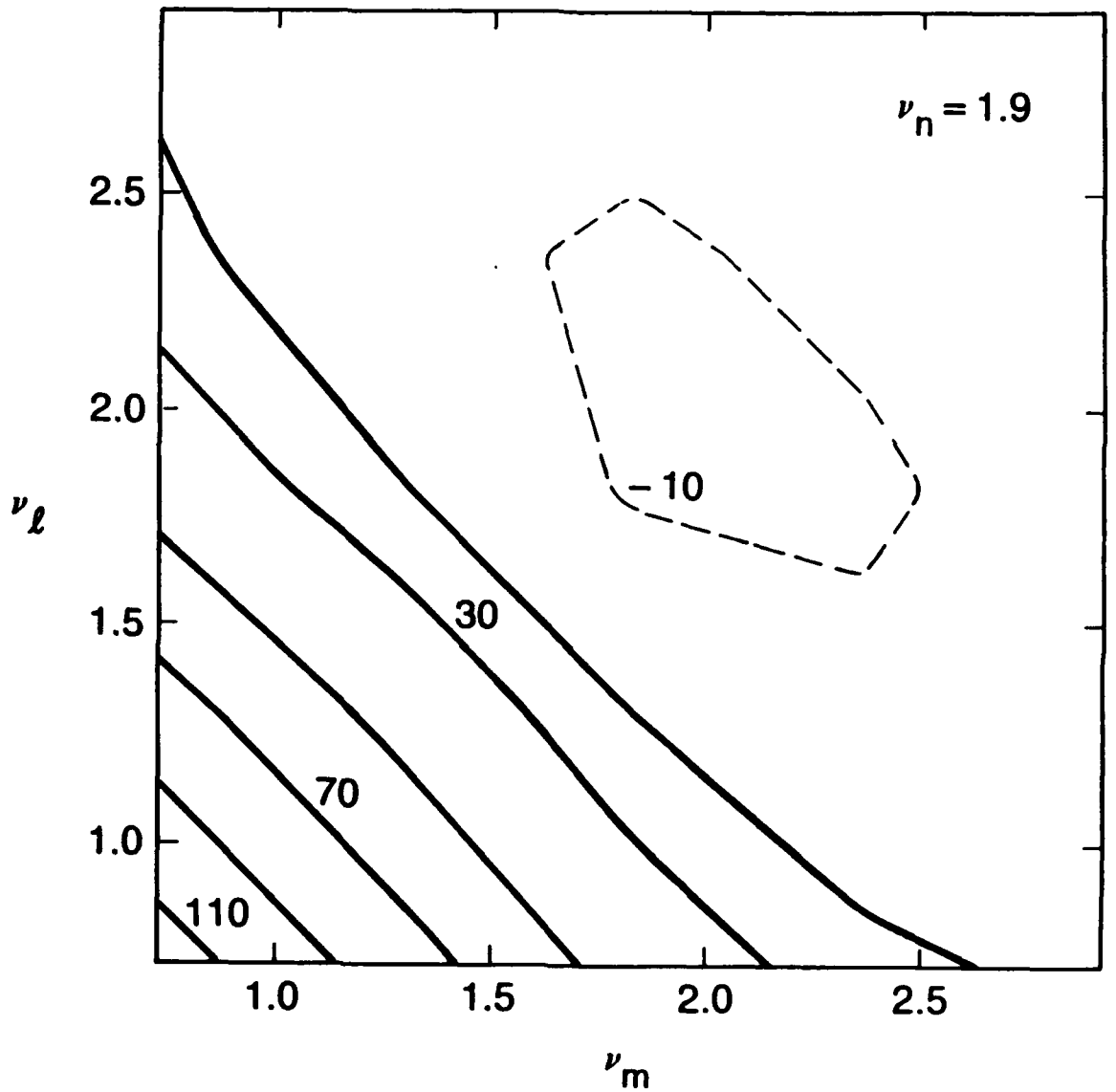

(b)

Fig. 4 (Continued) — Contour plots for the real parts of the fifth order coupling coefficients $\hat{D}_{nlm}$ on the ν_n = const. plane for (a) $\nu_n = 0.8$ (b) $\nu_n = 1.9$ (c) $\nu_n = 2.9$. The contour plots in (d) are drawn for $\nu_m = \nu_l$.

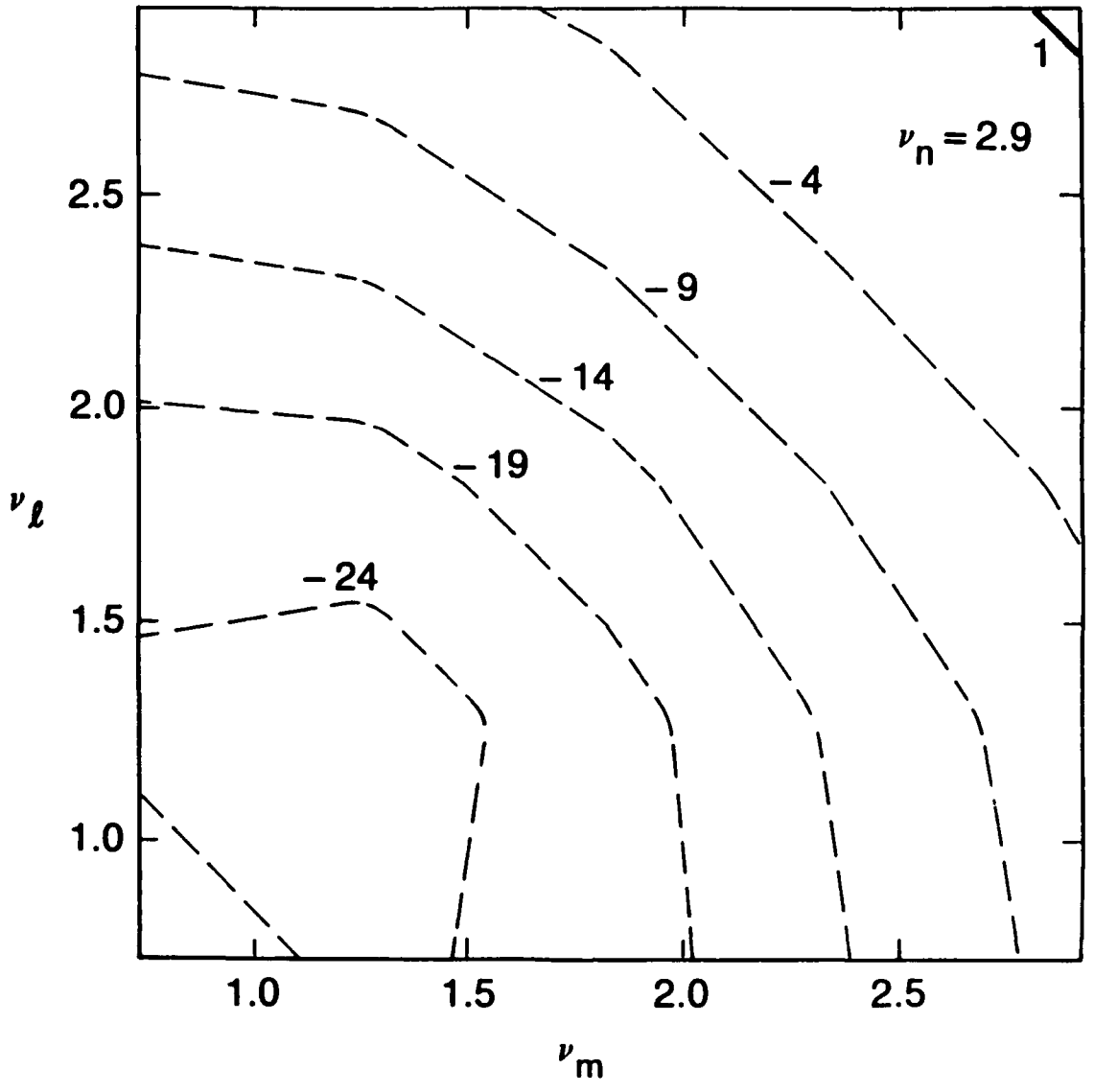

(c)

Fig. 4 (Continued) — Contour plots for the real parts of the fifth order coupling coefficients $\hat{D}_{nlm}$ on the ν_n = const. plane for (a) $\nu_n = 0.8$ (b) $\nu_n = 1.9$ (c) $\nu_n = 2.9$. The contour plots in (d) are drawn for $\nu_m = \nu_l$.

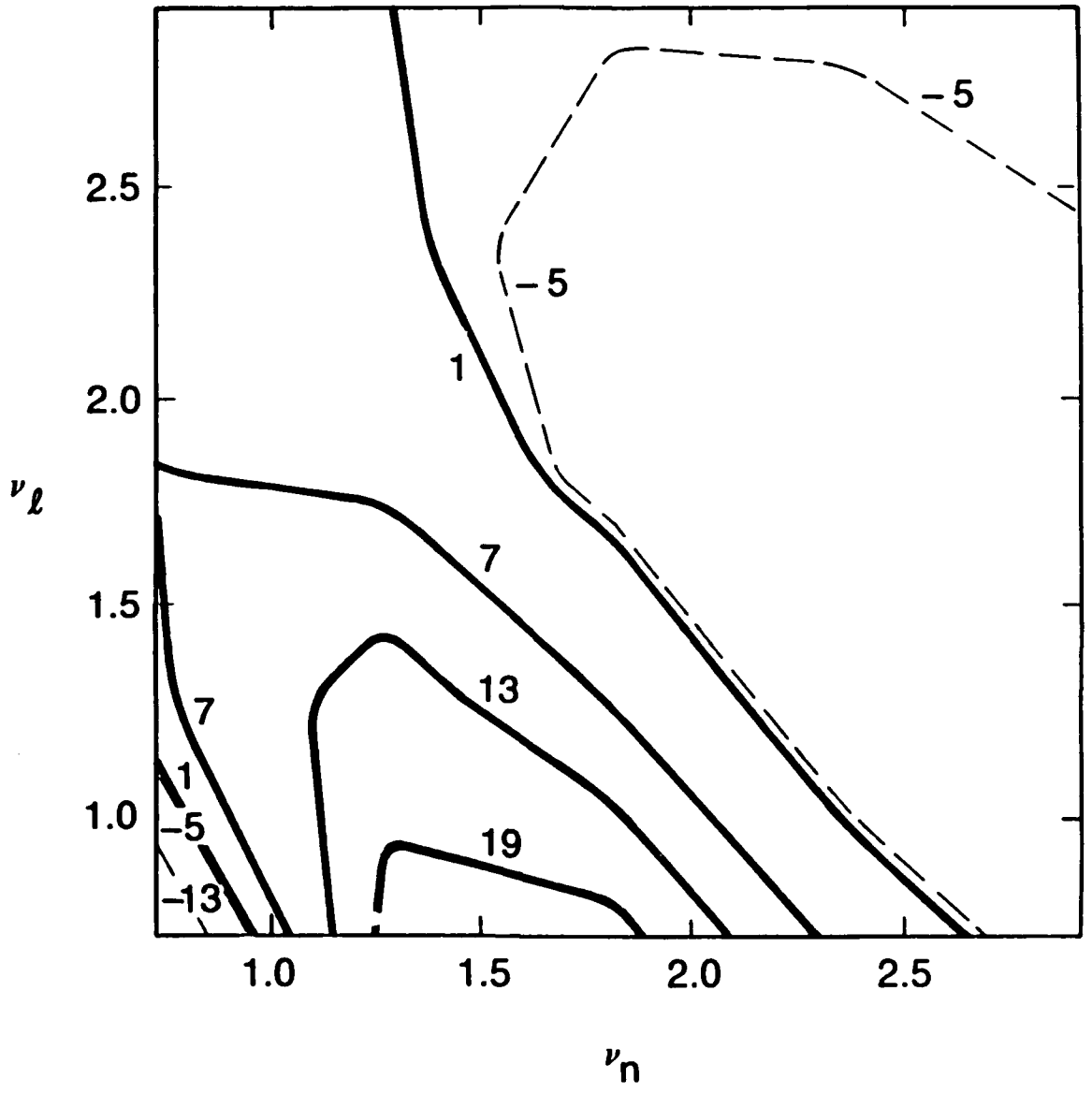

(d)

Fig. 4 (Continued) — Contour plots for the real parts of the fifth order coupling coefficients $\hat{D}_{nlm}$ on the ν_n = const. plane for (a) $\nu_n = 0.8$ (b) $\nu_n = 1.9$ (c) $\nu_n = 2.9$. The contour plots in (d) are drawn for $\nu_m = \nu_1$.

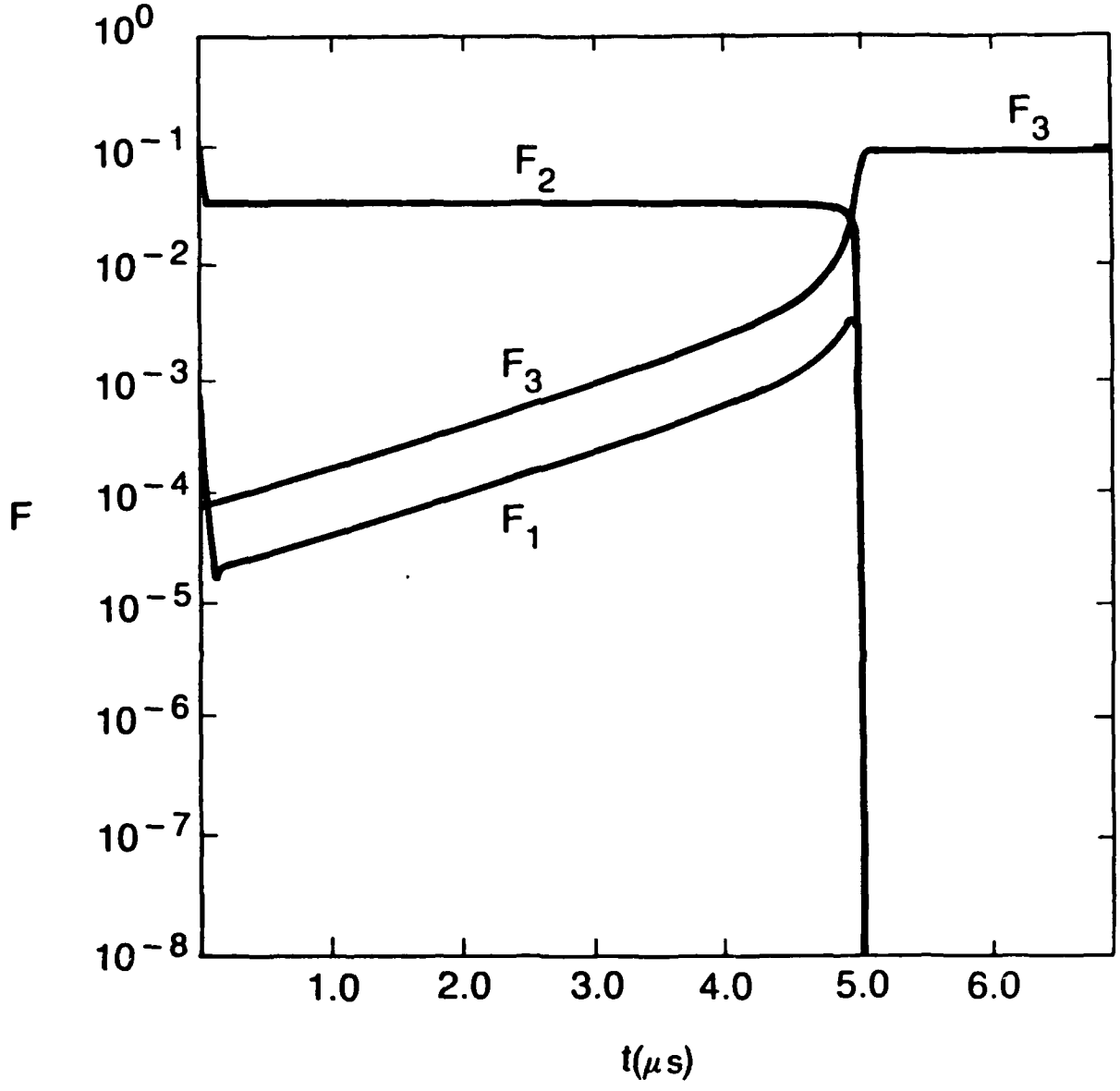

(a)

Fig. 5 — Mode competition in the QOG for the first three modes above ω_o. The time evolution of the amplitudes F in (a)-(c) corresponds to different initial conditions.

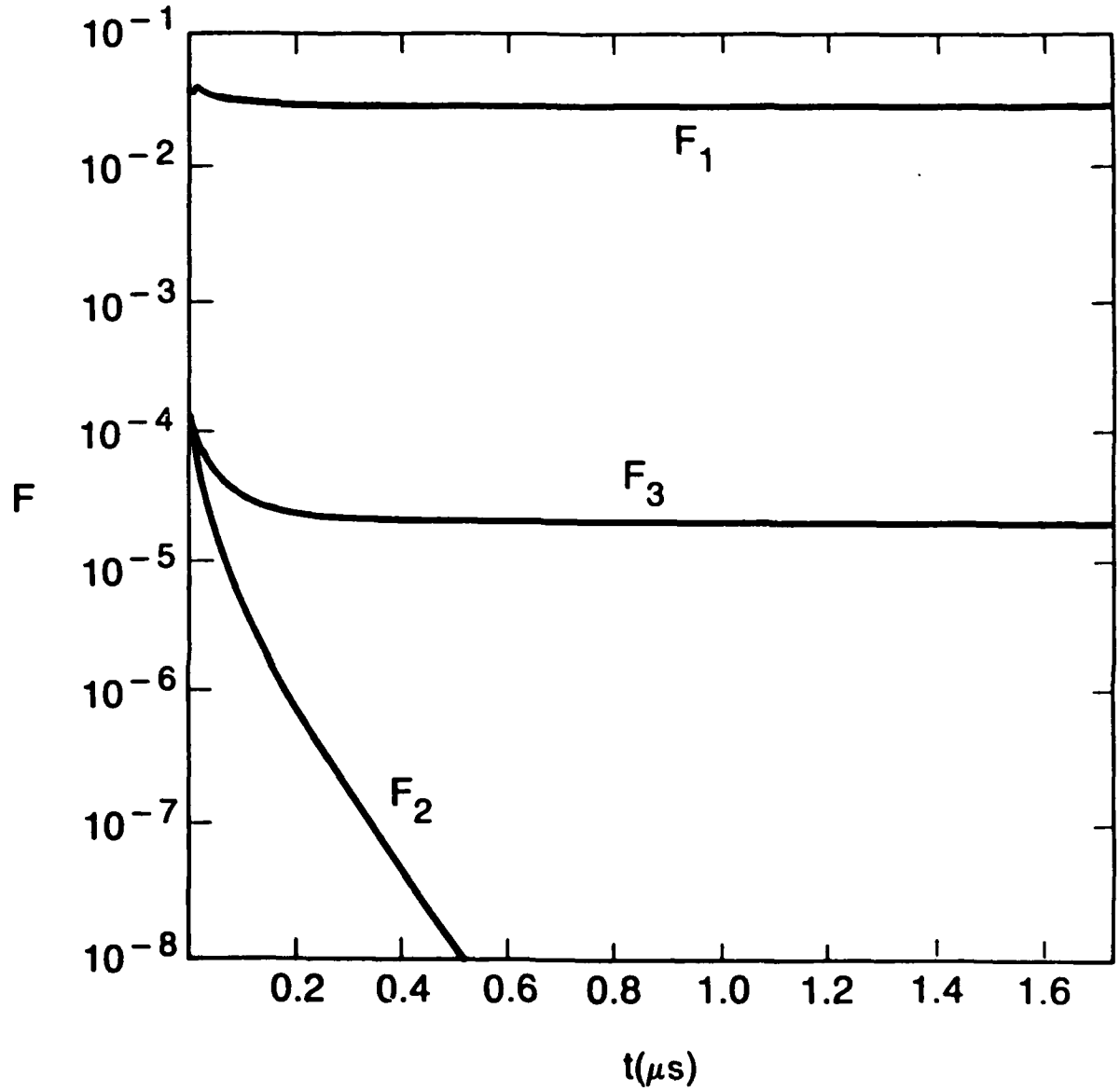

(b)

Fig. 5 (Continued) — Mode competition in the QOG for the first three modes above ω_o. The time evolution of the amplitudes F in (a)-(c) corresponds to different initial conditions.

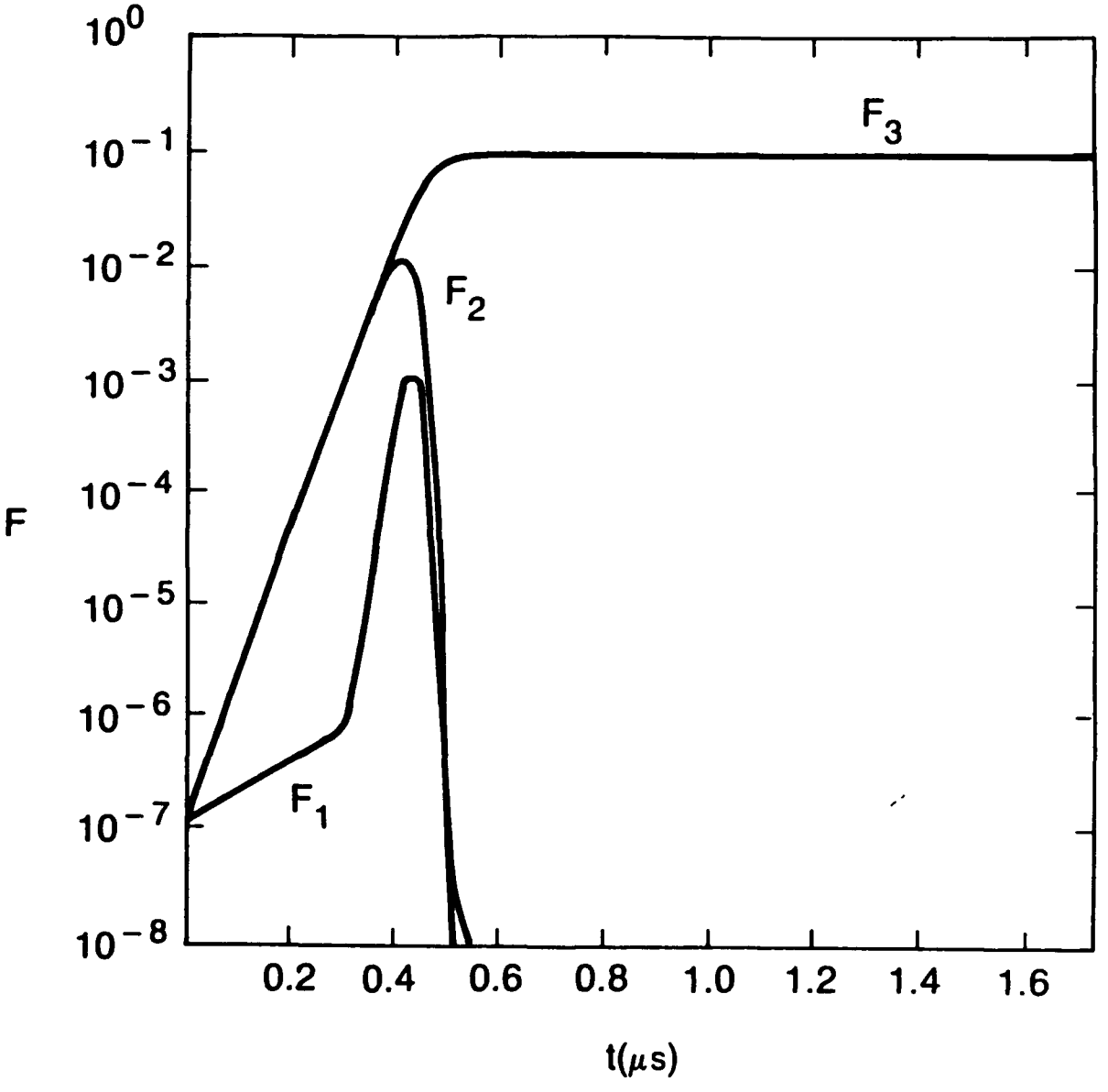

(c)

Fig. 5 (Continued) — Mode competition in the QOG for the first three modes above ω_o. The time evolution of the amplitudes F in (a)-(c) corresponds to different initial conditions.

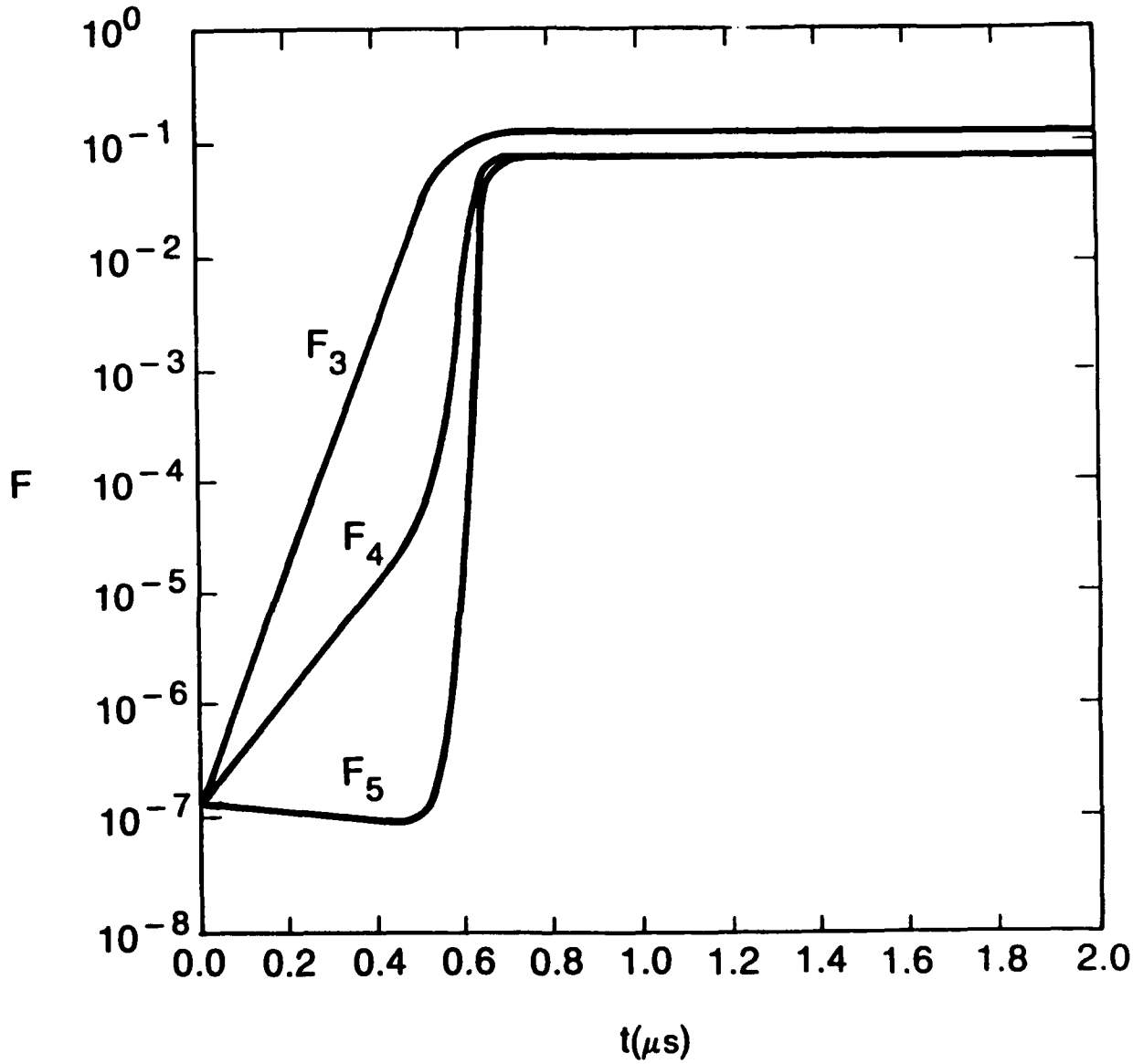

Fig. 6 — Mode competition among the third, fourth and fifth modes for same parameters as in Fig. 5.

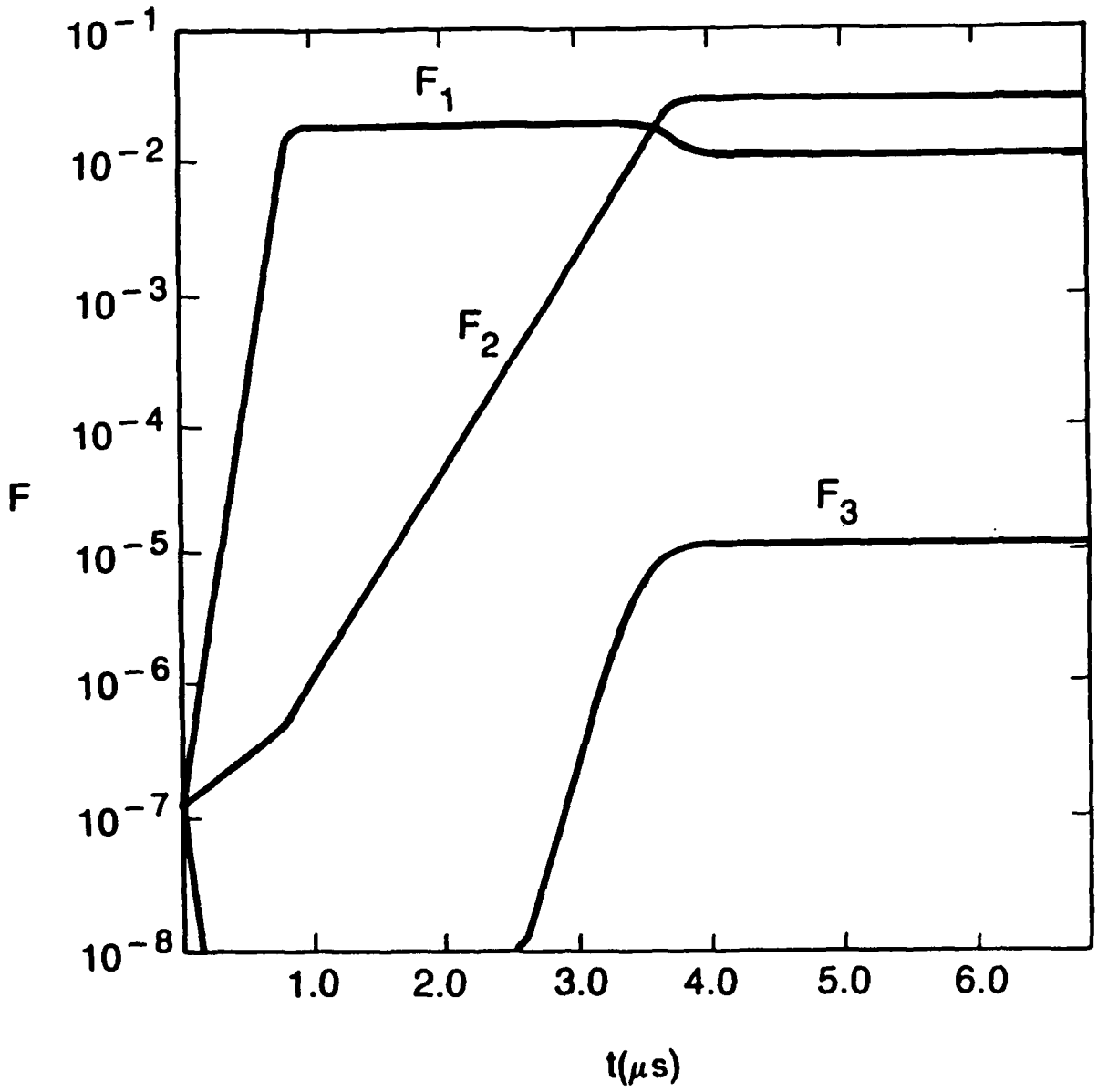

Fig. 7 — Mode competition among the first three modes in a cavity of half the length and same other parameters as in Figs. 5 and 6

4793/4 DISTRIBUTION LIST
Updated 2 Aug 89

Air Force Avionics Laboratory AFWAL/AADM-1 Wright/Patterson AFB, OH 45433 Attn: Walter Friez	1 copy
Air Force Office of Scientific Research Bolling AFB Washington, D.C. 20332 Attn: H. Schlossberg	1 copy
Air Force Weapons Lab Kirkland AFB Albuquerque, NM 87117-6008 Attn: Dr. William Baker Dr. Brendon Godfrey	2 copies 1 copy
Bhabha Atomic Research Center Laser Division Bombay, India 400085 Attn: T.S. Shirsat	1 copy
Columbia University 520 West 120th Street Department of Electrical Engineering New York, NY 10027 Attn: Dr. S.P. Schlesinger A. Sen	1 copy 1 copy
Columbia University 520 West 120th Street Department of Applied Physics and Nuclear Engineering New York, NY 10027 Attn: T.C. Marshall R. Gross	1 copy 1 copy
Cornell University School of Applied and Engineering Physics Ithica, NY 14853 Attn: Prof. Hans H. Fleischmann John Nation R. N. Sudan	1 copy 1 copy 1 copy
Creol-FEL Research Pavillion 12424 Research Parkway, Suite 400 Orlando, FL 32826 Attn: Dr. Luis R. Elias Dr. I. Kimel	1 copy 1 copy

Dartmouth College
18 Wilder, Box 6127
Hanover, NH 03755
Attn: Dr. John E. Walsh — 1 copy

Defense Advanced Research Project Agency/DEO
1400 Wilson Blvd.
Arlington, VA 22209
Attn: Dr. L. Buchanan — 1 copy

Defense Communications Agency
Washington, D.C. 20305
Attn: Dr. Pravin C. Jain
Assistant for Communications
Technology — 1 copy

Defense Nuclear Agency
Washington, D.C. 20305
Attn: Mr. J. Farber — 1 copy
Dr. Leon Wittwer (RAAE) — 5 copies

Defense Technical Information Center
Cameron Station
5010 Duke Street
Alexandria, VA 22314 — 2 copies

Department of Energy
Div. of Advanced Energy Projects
Washington, DC 20545
Attn: Dr. R. Gajewski — 1 copy

Department of Energy
Office of Energy Research
Washington, D.C. 20545
Attn: C. Finfgeld/ER-542, GTN — 1 copy
T.V. George/ER-531, GTN — 1 copy
D. Crandall/ER-54, GTN — 1 copy
Dr. David F. Sutter/ER-224, GTN — 1 copy

Director of Research
U. S. Naval Academy
Annapolis, MD 21402-5021 — 1 copy

General Atomics
13-260
Box 85608
San Diego, CA 92138
ATTN: Dr. J. Doane — 1 copy
Dr. C. Moeller — 1 copy

Georgia Tech. EES-EOD
Baker Building
Atlanta, GA 30332
Attn: Dr. James J. Gallagher — 1 copy

Hanscomb Air Force Base
Stop 21, MA 01731
Attn: Lt. Rich Nielson/ESD/INK — 1 copy

Hughes Aircraft Co.
Electron Dynamics Division
3100 West Lomita Boulevard
Torrance, CA 90509
Attn: J. Christiansen — 1 copy
J. Tancredi — 1 copy

Hughes Research Laboratory
3011 Malibu Canyon Road
Malibu, CA 90265
Attn: Dr. R. Harvey — 1 copy
Dr. R.W. Schumacher — 1 copy

KMS Fusion, Inc.
3941 Research Park Dr.
P.O. Box 1567
Ann Arbor, MI 48106
Attn: S.B. Segall — 1 copy

Lawrence Berkeley Laboratory
University of California
1 Cyclotron road
Berkeley, CA 94720
Attn: Dr. A.M. Sessler — 1 copy

Lawrence Livermore National Laboratory
P.O. Box 808
Livermore, CA 94550
Attn: Dr. D. Prosnitz — 1 copy
Dr. T.J. Orzechowski — 1 copy
Dr. J. Chase — 1 copy
Dr. W.A. Barletta — 1 copy
Dr. D.L. Birx — 1 copy
Dr. E.T. Scharlemann — 1 copy

Litton Electron Devices
960 Industrial Road
San Carlos, CA 94070
Attn: Library — 1 copy

Los Alamos National Scientific Laboratroy
P.O. Box 1663, MSJ 564
Los Alamos, NM 87545
Attn: Dr. Brian Newman — 1 copy

Los Alamos Scientific Laboratory
P.O. Box 1663, AT5-827
Los Alamos, NM 87545
Attn: Dr. T.J.T. Kwan — 1 copy
Dr. L. Thode — 1 copy
Dr. C. Brau — 1 copy
Dr. R. R. Bartsch — 1 copy

Massachusetts Institute of Technology
Department of Physics
Cambridge, MA 02139
Attn: Dr. G. Bekefi/36-213 — 1 copy
Dr. M. Porkolab/NW 36-213 — 1 copy
Dr. R. Davidson/NW 16-206 — 1 copy
Dr. A. Bers/NW 38-260 — 1 copy
Dr. K. Kreischer — 1 copy
Dr. B. Danby — 1 copy
Dr. G.L. Johnston — 1 copy

Massachusetts Institute of Technology
167 Albany St., N.W. 16-200
Cambridge, MA 02139
Attn: Dr. R. Temkin/NW 14-4107 — 1 copy

Mission Research Corporation
8560 Cinderbed Road, Suite 700
Newington, VA 22122
Attn: Dr. M. Bollen — 1 copy

Dr. J. Pasour — 1 copy

Naval Research Laboratory
Addressee: Attn: Name/Code
Code 0124 - ONR — 1 copy
Code 1000 - Commanding Officer — 1 copy
Code 1001 - T. Coffey — 1 copy
Code 1003.9A - Computer Resources Architect — 1 copy
Code 1005 - Head, Office of Mgt. & Admin. — 1 copy
Code 1005.1 - Deputy Head, Off. of Mgt. & Admin. — 1 copy
Code 1005.6 - Head, Directives Staff — 1 copy
Code 1200 - Capt. R. W. Michaux — 1 copy
Code 1201 - Deputy Head, Command Support Division — 1 copy
Code 1220 - Security — 1 copy
Code 2000 - J. Brown — 1 copy
Code 2604 - NRL Historian — 1 copy
Code 2628 - TID Distribution — 22 copies
Code 2634 - Cindy Sims — 1 copy
Code 3000 - R. Doak — 1 copy

Code 4000 - W. Ellis	1 copy
Code 4600 - D. Nagel	1 copy
Code 4700 - S. Ossakow	26 copies
Code 4780.1 - W. Ali	1 copy
Code 4790 - Branch Office	4 copies
Code 4794/4793 - Library	20 copies
Code 4793 - W. Black	1 copy
Code 4770 - G. Cooperstein	1 copy
Code 4794 - A. Fliflet	1 copy
Code 4793 - S. Gold	1 copy
Code 4790 - C. Hui	1 copy
Code 4795 - C. Kapetanakos	1 copy
Code 4793 - A. Kinkead	1 copy
Code 4790 - Y. Lau	1 copy
Code 4707 - W. Manheimer	1 copy
Code 4794 - M. Rhinewine	1 copy
Code 4790 - P. Sprangle	1 copy
Code 5700 - L. Cosby	1 copy
Code 6840 - S. Ahn	1 copy
Code 6840 - A. Ganguly	1 copy
Code 6840 - R. Parker	1 copy
Code 6840 - N. Vanderplaats	1 copy
Code 6850 - L. Whicker	1 copy
Code 6875 - R. Wagner	1 copy

Naval Sea Systems Command
Department of the Navy
Washington, D.C. 20362
Attn: Commander, PMS 405-300 — 1 copy

Northrop Corporation
Defense Systems Division
600 Hicks Rd.
Rolling Meadows, IL 60008
Attn: Dr. Gunter Dohler — 1 copy

Oak Ridge National Laboratory
P.O. Box Y
Mail Stop 3
Building 9201-2
Oak Ridge, TN 37830
Attn: Dr. A. England — 1 copy

Office of Naval Research
800 N. Quincy Street
Arlington, VA 22217
Attn: Dr. C. Roberson — 1 copy

Office of Naval Research
1012 W 36th Street, Childs Way Bldg.
Los Angeles, CA 90089-1022
Attn: Dr. R. Behringer — 1 Copy

Optical Sciences Center
University of Arizona
Tucson, AZ 85721
Attn: Dr. Willis E. Lamb, Jr. — 1 copy

Physical Sciences, Inc.
635 Slaters Lane #G101
Alexandria, VA 22314-1112
ATTN: Dr. M.E. Read — 1 copy

Physics International
2700 Merced Street
San Leandro, CA 94577
Attn: Dr. J. Benford — 1 copy

Princeton Plasma
Plasma Physics Laboratory
James Forrestal Campus
P.O. Box 451
Princeton, NJ 08544
Attn: Dr. H. Hsuan — 2 copies
Dr. D. Ignat — 1 copy
Dr. H. Furth — 1 copy
Dr. P. Efthimion — 1 copy
Dr. F. Perkins — 1 copy

Raytheon Company
Microwave Power Tube Division
Foundry Avenue
Waltham, MA 02154
Attn: N. Dionne — 1 copy

Sandia National Laboratories
ORG. 1231, P.O. Box 5800
Albuquerque, NM 87185
Attn: Dr. Thomas P. Wright — 1 copy
Mr. J.E. Powell — 1 copy
Dr. J. Hoffman — 1 copy
Dr. W.P. Ballard — 1 copy
Dr. C. Clark — 1 copy

Science Applications, Inc.
1710 Goodridge Dr.
McLean, VA 22102
Attn: Adam Drobot — 1 copy
P. Vitello — 1 copy
D. Bacon — 1 copy
C. Menyuk — 1 copy

Science Research Laboratory
15 Ward Street
Somerville, MA 02143
Attn: Dr. R. Shefer — 1 copy

SPAWAR
Washington, D.C. 20363
Attn: E. Warden, Code PDE 106-3113 — 1 copy
Capt. Fontana, PMW 145 — 1 copy

Spectra Technologies
2755 Northup Way
Bellevue, WA 98004
Attn: Dr. J.M. Slater — 1 copy

Stanford University
Dept. of Electrical Engineering
Stanford, CA 94305
Attn: Dr. J. Feinstein — 1 copy

Stanford University
High Energy Physics Laboratory
Stanford, CA 94305
Attn: Dr. T.I. Smith — 1 copy

TRW, Inc.
One Space Park
Redondo Beach, CA 90278
Attn: Dr. H. Boehmer — 1 copy
Dr. T. Romisser — 1 copy
Dr. Z. Guiragossian — 1 copy

University of California
Physics Department
Irvine, CA 92717
Attn: Dr. G. Benford — 1 copy
Dr. N. Rostoker — 1 copy

University of California
Department of Physics
Los Angeles, CA 90024
Attn: Dr. A.T. Lin — 1 copy
Dr. N. Luhmann — 1 copy
Dr. D. McDermott — 1 copy

University of Maryland
Department of Electrical Engineering
College Park, MD 20742
Attn: Dr. V. L. Granatstein — 1 copy
Dr. W. W. Destler — 1 copy

University of Maryland
Laboratory for Plasma and Fusion
Energy Studies
College Park, MD 20742

Attn:	Dr. Tom Antonsen	1 copy
	Dr. John Finn	1 copy
	Dr. Jhan Varyan Hellman	1 copy
	Dr. W. Lawson	1 copy
	Dr. Baruch Levush	1 copy
	Dr. Edward Ott	1 copy
	Dr. M. Reiser	1 copy

University of New Mexico
Department of Physics and Astronomy
800 Yale Blvd, N.E.
Albuquerque, NM 87131

Attn:	Dr. Gerald T. Moore	1 copy

University of Tennessee
Dept. of Electrical Engr.
Knoxville, TN 37916

Attn:	Dr. I. Alexeff	1 copy

University of Utah
Department of Electrical Engineering
3053 Merrill Engineering Bldg.
Salt Lake City, UT 84112

Attn:	Dr. Larry Barnett	1 copy
	Dr. J. Mark Baird	1 copy

U. S. Army
Harry Diamond Labs
2800 Powder Mill Road
Adelphi, MD 20783-1145

Attn:	Dr. Howard Brandt	1 copy
	Dr. Edward Brown	1 copy
	Dr. Stuart Graybill	1 copy
	Dr. A. Kehs	1 copy
	Dr. J. Silverstein	1 copy

Varian Associates
611 Hansen Way
Palo Alto, CA 94303

Attn:	Dr. H. Huey	1 copy
	Dr. H. Jory	1 copy
	Dr. Kevin Felch	1 copy
	Dr. R. Pendleton	1 copy
	Dr. A. Salop	1 copy

Varian Eimac San Carlos Division
301 Industrial Way
San Carlos, CA 94070

Attn:	C. Marshall Loring	1 copy

Yale University
Applied Physics
Madison Laboratory
P.O. Box 2159
Yale Station
New Haven, CN 06520
Attn: Dr. I. Bernstein

Ken Busby

Director of Research
U.S. Naval Academy
Annapolis, MD 21402
(2 copies)

Do NOT make labels for
Records----(01 cy)

Naval Research Laboratory
Washington, DC 20375-5000
Code 2630
Timothy Calderwood